CERAMIC MATERIALS MIMICKING NORMAL BONE SURFACE MICROSTRUCTURE AND CHEMISTRY MODULATE OSTEOBLAST RESPONSE

A Dissertation
Presented to
The Academic Faculty

By

Brandy Rogers Adams

In Partial Fulfillment
of the Requirements for the Degree
Doctor of Philosophy in the
School of Biomedical Engineering

Georgia Institute of Technology
December 2013

CERAMIC MATERIALS MIMICKING NORMAL BONE SURFACE MICROSTRUCTURE AND CHEMISTRY MODULATE OSTEOBLAST RESPONSE

Approved by:

Dr. Barbara D. Boyan, Advisor
School of Engineering
Georgia Institute of Technology,
Virginia Commonwealth University

Dr. Kenneth H. Sandhage
School of Materials Science & Engineering
Georgia Institute of Technology

Dr. Zvi. Schwartz
School of Engineering
Virginia Commonwealth University

Dr. Laurie Gower
School of Materials Science & Engineering
University of Florida

Dr. Julia Babensee
School of Biomedical Engineering
Georgia Institute of Technology

Date Approved: June 27, 2013

DEDICATION

"To whom much is given, much is required." This dissertation is dedicated to my loved ones because I could not have completed my doctorate without the help of God, family, and friends who have encouraged me at every stage of this journey. My grandmother, Letha Mae Daniel, was the valedictorian of her high school class and received a full scholarship to Alabama State University (ASU) in the 1940's. Although she never matriculated at ASU, it was her love for family and education that motivated her to ensure that her three children attended and graduated from college. If it were not for this legacy of love, encouragement, and strong will, I would not have dreamed of embarking upon such a challenging endeavor as obtaining a doctorate. My mother, Doretha Rogers, continues to be my greatest supporter and role model. My mother is a true an example of the character, strength, and selfless love that I aspire to emulate. My older sisters, Tracy and Jocelyn, continue to be my greatest confidants, counselors, and life coaches. They have always set the bar high for academic and career successes and I am grateful that they have helped me navigate my path. My father, Johnny Rogers, and brother, Rod, have been constant supporters who always remind me to "stay the course." I have a host of friends and sorors of Delta Sigma Theta who have always believed I could accomplish anything. My dearest friend, LaShawnda, has been more like family and always extended her hospitality and support wherever needed. Last, but far from least, my best friend, courageous soldier, and husband, Lee Adams, joined me in this journey mid-way through and has run this race with me, helping me to overcome all of its obstacles. His continued confidence in me has motivated me to overcome my fears and complete this journey.

With God all things are possible. My faith, perseverance, and expectation for God's goodness increased during this journey. I do not believe that we are blessed with God's gifts to enjoy them singularly, but instead we should share them with others. I would also like to share this dissertation with a young man, LaDarius Vaughn, that aspired to be a forensic scientist before passing at the age of fifteen. I hope that my achievements motivated him and continue to motivate the young people in my life to reach their greatest potential.

ACKNOWLEDGEMENTS

This research was directed by my thesis advisor Dr. Barbara Boyan and research advisor Dr. Zvi Schwartz of Virginia Commonwealth University in Richmond, Virginia. Material contributions were provided by Dr. Amany Mostafa of the National Research Center in Cairo, Egypt and Dr. Laurie Gower of the University of Florida in Gainesville, Florida. This research was funded in part by an NSF NIRT grant BES-0404000 (LG) and NIH grant AR052102 (BDB).

TABLE OF CONTENTS

LIST OF FIGURES

LIST OF ABBREVIATIONS

MCB	Mineralized cortical bone
PDCB	Partially demineralized cortical bone
FDCB	Fully demineralized cortical bone
MTB	Mineralized trabecular bone
PDTM	Partially demineralized trabecular bone
FDTB	Fully demineralized trabecular bone
HA	Hydroxyapatite
CO_3^{2-}HA	Carbonated hydroxyapatite
Si-HA	Silicated hydroxyapatite
PILP	Polymer-induced liquid precursor
CS	Collagen sponge
CSHA	Collagen sponge mineralized w/o PILP
CSPILP	Collagen sponge mineralized with PILP
$\alpha 2\beta 1$	Alpha2, beta1integrin

SUMMARY

Bone consists of collagen/hydroxyapatite (HA) composites in which poorly crystalline carbonated calcium phosphate is intercalated within the fibrillar structure. Normal bone mineral is a carbonated-apatite, but there are limited data on the effect of mineral containing carbonate on cell response. Although the exact biological role of silicate in bone formation is unclear, silicate has been identified at trace levels in immature bone and is believed to play a metabolic role in new bone formation. To mimic the inorganic and organic composition of bone we have developed a variety of bone graft substitutes. In the present body of research, we characterized the surface composition of human cortical and trabecular bone. When then characterized the surface compositions of the following potential bone substitutes: carbonated hydroxyapatite (CO_3^{2}-HA), silicated hydroxyapatite (Si-HA), and collagen sponges mineralized with calcium phosphate using the polymer-induced liquid-precursor (PILP) process. In the latter substitutes, the PILP process leads to type I collagen fibrils infiltrated with an amorphous mineral precursor upon which crystallization leads to intrafibrillar HA closely mimicking physiological bone mineral. We then determined the osteoblast-like cell response to each bone substitute to characterize the substrate's effect on osteoblast differentiation. The observations collectively indicate that cells are sensitive to the formatting of the mineral phase of a bone substitute and that this format can be altered to modulate cell behavior.

CHAPTER 1

1.1 Introduction

The premise of this dissertation is to investigate and develop a fundamental understanding of the chemical and structural presentation of bone and determine whether this presentation has a significant role in the development of new bone. The various components of bone have been explored and characterized in previous studies. The primary focus of this body of research is to determine whether the inorganic and organic presentation of bone modulates the formation of new bone so that this understanding can be incorporated into the design of sustainable bone substitutes. Bone also undergoes resorbtion prior to the formation of new bone. The structural and chemical presentation of bone may also play a significant role in facilitating bone resorbtion, however, we did not examine this aspect of bone development in the present work.

Biomaterials chemically and physically address the issue of segmental bone defects by serving as a medium to either recover damaged bone due to pathological malfunction or replace bone loss due to a traumatic injury. The biomaterials industry encompasses a large sector focused on designing and developing bone substitutes to meet these needs. This growing industry is aggressively yielding products that both chemically and mechanically mimic physiological bone, while at the same time encouraging the formation of new bone. Traumatic injury to bone resulting in a segmental defect, and the deterioration of bone due to disease, continuously creates a need for readily available bone graft substitutes. Autologous bone is by far the most effective bone graft material owing to its intrinsic osteoconductive and osteoinductive properties. Donor site morbidity

and limited availability, however, especially in adolescents, presents serious challenges for its use, and thus drives the demand for the developing biological materials and substitutes.

It is well known that injury to, or disease of, the architecture of bone, greatly impedes the body's mobility and cripples its defense, thereby disrupting the body's overall homeostasis. Millions of people experience injuries to various skeletal bones while performing routine activities. At the same time, several bone infections and diseases such as osteoporosis, osteogenesis imperfecta, rickets and osteomyelitis compromise the integrity of bone, debilitating people yearly. According to the American Society of Clinical Oncology, in 2013 an estimated 3,010 cases of bone cancers will be diagnosed whereas in 2010 there were approximately 2,650 cases. Of these estimated cases for this year, 1,440 are believed to result in deaths, whereas in 2010 the reported cases resulted in 1,460 deaths in the U.S. alone (Cancer.org). In order to prevent complete loss of function, unhealthy bone must be restored or replaced, while the formation of new bone is encouraged. Therefore, bone biomaterials that mimic physiological bone are an ideal solution for the replacement of unhealthy bone and its restoration through the formation of new healthy bone.

A number of materials have been evaluated to determine their success and compatibility as potential bone graft substitutes. Synthetic bioactive glass, ceramics, coral, and calcium phosphate powders are some of those researched and developed as viable bone substitutes. An essential characteristic of a successful bone graft material is the attachment and proliferation of osteogenic cells onto the substitute surface. Once osteogenic cells attach to the substitute surface, osseointegration between the material

and physiological bone is necessary for successful replacement of defective tissue and generation of new bone.

Today's tissue engineered bone substitute's principal role is the stimulation of autogenous bone in concert with the resorption of the scaffolding material, and not the permanent residency of the bone replacement. There are numerous physiological advantages for using bone substitutes when the biomaterials meet these requirements. These advantages include, but are not limited to, their ability to encourage growth and differentiation of osteogenic cells, their stimulation of angiogenesis to support these differentiated cells and newly formed tissue, as well as the substitute's potential for mass production. In this ever-evolving tissue engineering arena, the design and development of biomaterials that functionally mimic the chemical composition and micro-architecture of physiological bone is of great necessity and in great demand. With this in mind, we hypothesize that ceramic materials mimicking normal bone surface microstructure and chemistry will support an increase in osteoblast differentiation in vitro. The characterization of these materials and the evaluation of the response osteoblast-like cell to these biomaterials is the underlying premise of this work.

1.2 Background and Significance

1.2.1 Bone

Giving form to the body, supporting tissues and permitting movement by providing points of attachment for muscles, are but a few of bone's many functions. Bone is not only the backbone of the body's endoskeleton system, but is a metabolically active organ with many functions that are critical to the body's homeostasis, such as protecting many of the body's vital organs [1]. In addition to these functions, bone plays a crucial

role in mineral homeostasis, storing minerals such as calcium, phosphate, carbonate, silicate, and magnesium that are essential for many cellular mechanisms.

1.2.2 Bone Cells

Bone is a dynamic tissue that is continuously being remodeled and formed. There are three different types of cells that facilitate bone's ability to grow, repair itself, change shape and synthesize (osteoblast) new osseous tissue and resorb (osteoclast) old tissue [2]. The primary function of osteoblasts is to synthesize the organic matrix components of bone and assist in the mineralization of this tissue. Osteoclast cells resorb both the mineral and the organic phases of bone. Osteocytes are osteoblast cells that have become imprisoned within the mineralized bone matrix [2]. Their role in mineral and organic element homeostasis is not well defined. Osteoblast and osteoclast work in tandem, resulting in a coupling process that supports the remodeling and maintenance of bone [1].

1.2.3 Bone Components

It is well known that bone is a mineralized connective tissue composed of both organic and inorganic components. The mineral phase of bone constitutes about two-thirds of its weight, while the remaining third is an organic matrix, primarily consisting of collagen and small amounts of proteoglycan, lipid, and several noncollagenous proteins [3]. $Ca_{10}(PO_4)_6(OH)_2$, more commonly known as hydroxyapatite (HA), is chemically similar to the major mineral component of bone, which comprises approximately 70% of this mineralized tissue [4]. Previous studies report calcium phosphate powders as biocompatible substitutes when interfacing with osteogenic cells, as a result of their osteoconductive and osteoinductive properties [5]. Consequently, calcium phosphates are

used to coat many grafts and substitutes, in hopes of encouraging osseointegration of an implant or substitute. Hydroxyapatite is one of the few materials identified as bioactive, as it will support bone ingrowth and osseointegration when used in orthopedic, dental and maxillofacial applications [4].

1.2.4 Biomineral

Crystalline carbonated hydroxylapatite is the naturally occurring biomineral apatite found in bone. The carbonate content of biomineral is approximately 2-8wt%, depending upon the age of the individual [6]. A major focus of biomaterials research is the preparation of synthetic carbonate containing hydroxyapatite bioceramics that resemble the chemical composition of bone [7]. Hydroxyapatite is a bioactive material, when implanted *in vivo*, which is able to interact with the host by bonding to tissue, stimulating a biological response at the host and biomaterial interface. In hopes of mimicking carbonated biomineral hydroxyapatite, synthetic carbonated hydroxyapatite can be simulated by incorporating carbonate ions into the hydroxyapatite lattice structure, replacing both the hydroxyl and phosphate ions [4]. Replacing the hydroxyl group gives rise to a type-A substitution, while replacement of the phosphate group yields type-B carbonation. A-B type carbonation represents the physiological carbonate hydroxyapatite and can be achieved by substituting carbonate ions into both the phosphate and hydroxyl groups [8-9]. As a biomaterial, carbonate substituted hydroxyapatite having a carbonate concentration within the physiological range, has great potential as a bone replacement filler of both load-bearing and non-load bearing osseous defects [10]. When integrated into existing osseous tissue, this substitute can encourage the formation of new bone. Evaluating various carbonate ionic concentrations within the hydroxyapatite lattice,

increases the potential determining an optimal carbonate concentration necessary to produce a biologically effective bone substitute.

1.2.5 Select Ionic Insertions

Ionic substitution of carbonate or insertion of silicate is likely to affect hydroxyapatite's surface structure, surface charge, and solubility, which will all have an effect on hydroxyapatite's biological performance *in vitro* and *in vivo* [11]. Approximately two-thirds of physiological bone is composed of carbonated hydroxyapatite. Carbonated HA substitutes therefore have the ability to chemically represent and mimic native bone. In addition to carbonate, silicon is recognized as playing a major role in the initial stages of bone development when the protein matrix is constructed. It has been proposed that silicon may also increase the rate of bone mineralization and enhance calcium deposition in bone, allowing bone to develop faster and with greater integrity and mechanical strength [12, 13]. *In vitro* and *in vivo* studies by Carlisle [13] have shown that silicon was localized in active growth areas, such as the osteoid of young bone in rats and mice, where silicon levels of up to 0.5 wt% were observed. In bioactive glass, the formation of Si-OH bonds, the condensation and repolymerization of the SiO_2-rich layer on the surface of the glass, and the formation of a calcium phosphate layer on top of the SiO_2-rich layer, are all believed to initiate key mineralization and biological processes. These events lead to the subsequent crystallization of apatite crystals, cell adhesion, collagen formation, and protein adsorption. It is these processes that lead to the formation of an interfacial bonding zone between bone and bioactive glass *in vivo* [12].

1.2.6 Type I Collagen

Bone cells, collagen fibers, various growth factors, and several noncollagenous proteins all contribute to the organic phase of bone. Type I collagen is the paramount structural protein in bone's extracellular matrix and is the primary organic component of bone [14]. It assembles its tropocollagen units in a quarter-staggered array, which leads to hole and overlap zones that can be seen as periodic banding patterns. This quarter-stagger arrangement yields a regular array of 40 nm gaps within each periodic unit, and these are believed to be the locations where crystal nuclei are first observed [15]. A nanostructured array of hydroxyapatite hexagonal crystals, are embedded within the collagen matrix. Through intrafibrillar mineralization of collagen, an intimate relationship between self-assembled fibrillar collagen matrix and uniaxially oriented hydroxyapatite crystals is established and provides bone with its mechanical properties, strength, and ability to remodel [16]. It has been shown that parallel fibers of collagen mineralize in an intrafibrillar fashion in secondary bone formation [15]. Several modifications to this model have been proposed, such as the alignment of gaps to form grooves. These grooves are proposed to justify the occurrence of dimensions of HA crystals retrieved from bone that are larger than the dimensions of the gap zones where they are thought to form. The rod-like nature of the cylindrical tropocollagen units allows for collagen's crystalline character, which may play a role *in vivo* in the formation of tissues with intricate structural order [17]. This characteristic also accounts for mineral intrafibrillar infiltration and collagen spreading across lamellae in osteonal bone [18].

Commercially available bovine calcium phosphate ceramics have been used *in vivo* and *in vitro* applications and have exhibited excellent biocompatibility and

osteoconduction. Studies by Landi et al. [4] have demonstrated that the impregnation of cellulose sponges with HA powder suspension is effective in obtaining porous bodies with adequate pore dimensions and distribution. This bone substitute not only mimics the morphology of the spongy bone, but also lends itself to the osteoconduction process. Biomaterials incorporating both these organic and inorganic components of bone may best represent and manifest the chemical composition, mechanical strength and integrity of bone. These biomaterials may have clinical applications for the replacement of bone due to orthopedic defects, as well as maxillofacial, craniofacial, traumatic neck and head surgeries, and may provide solutions for generating new bone tissue with functional and mechanical qualities. Although there have only been a few scientific reports related to the association of bovine type I collagen to HA, combining these organic and inorganic components have previously been shown to enhance bone tissue formation in canine radial defects, in comparison to hydroxyapatite alone [19].

1.3 Specific Aims

Overall Hypothesis: Ceramic materials that mimic normal bone surface microstructure and chemistry will support an increase in osteoblast differentiation in vitro.

Experimental Hypothesis: Osteoblast behavior is dependent on the ceramic surface presentation.

1.3.1 Aim 1: To characterize the microstructure of normal bone surface.

Mineralized bovine bone wafers were partially and fully demineralized. The mineralized and demineralized resulting bone surface were characterized using scanning electron microscopy (SEM), energy dispersive X-ray spectroscopy (EDS), profilometry, X-ray photoelectron spectroscopy (XPS), and atomic force microscopy (AFM), contact angle,

and Fourier transform infrared spectroscopy (FT-IR). The surface characterizations of the mineralized bovine bone wafer were compared to both the partially and fully demineralized bone. Additionally, the characterizations of the microstructure of normal bone surface served as a native bone control for the characterization of ceramic materials mimicking normal bone surface microstructure and chemistry.

1.3.2 Aim 2: To determine whether ion substitution in hydroxyapatite affects osteoblast behavior.

Aim 2.1 – Material Characterization

Pure hydroxyapatite (HA) and substituted-HA surfaces were characterized using several material surface characterizations. SEM, EDS, XPS, profilometry, and the contact angle were determined to characterize each surface. In addition to these material characterizations, X-ray diffraction (XRD) was performed to determine if phase transitions occur in the material as a result of sintering, and to evaluate the surface's degree of crystallinity.

Aim 2.2 – *In vitro* Model

Carbonate and silicate substituted HA discs were used as the model system. HA powders containing carbonate or silicate with varying ion percent weights were pressed into 14mm discs. These discs were sintered for compactness and integrity, such that they would remain intact during cell culture. A firing schedule was developed to heat the discs from room temperature to 500°C at a 5 and 1°C/min rate and cooled similarly in order to prevent charring and/or cracking.

Aim 2.3 – Biological Assays

The ability of the ion substituted HA to affect osteoblast behavior was evaluated through a series of biological assays examining cell attachment, cell number, differentiation (alkaline phosphatase specific activity; osteocalcin protein), and local factor production (osteoprotegerin and vascular endothelial growth factor). The experiments used MG63 osteoblast-like human osteosarcoma cells.

1.3.3 Aim 3: To assess the effect of presentation of HA crystals within a collagen lattice on osteoblast behavior.

Aim 3.1 – Material Characterization

MG63 cells were cultured on model bovine type I collagen materials consisting of a commercially available bovine type I collagen sponge from ACE Surgical, Inc. or Collagen Matrix, Inc. HA crystals were incorporated into the material using a polymer induced liquid precursor (PILP) mineralization reaction and a non-PILP reaction. The PILP mineralization reaction uses an acidic polypeptide, polyaspartate to intrafibrillarly mineralize both collagen scaffold types. The non PILP mineralization does not add the polyaspartate, yielding a characteristic HA crystal hexagonal habit formation atop and around the collagen fibrils. The collagen scaffold surface was characterized using AFM, SEM, EDS, and TEM.

Aim 3.2 – *In vitro* Model

The collagen scaffolds were anchored to the bottom of 24 well-plates using a Cellcrown24 insert, consisting of a polycarbonate ring (Scaffdex, Inc.), in order to ensure full submergence within culture media during cell seeding and culturing. MG63 cells were grown to confluence and harvested for biological assays.

Aim 3.3 – Biological Assays

We assessed how PILP mineralization and non-PILP mineralization of collagen scaffolds with HA affect osteoblast behavior through evaluating a series of biological assays examining cell attachment, cell number, differentiation (alkaline phosphatase specific activity and osteocalcin protein), and local growth factor production (osteoprotegerin and vascular endothelial growth factor). Additionally, we assessed how behavior of α2-silenced MG63 cells, which have reduced α2β1 signaling, is modulated by non-PILP and PILP mineralized scaffolds; thereby evaluating the effect inorganic and organic presentation has on cell behavior.

1.4 References

[1] Freemont, A.J., "Basic bone cell biology," Int J Exp Pathol, 74(4), pp. 411-416 (1993).

[2] Huether, S.E., McCance, K.L., Understanding Pathophysiology. Second ed., St.Louis: Mosby (an imprint of Elsevier Science).

[3] Patel, N., Best, S.M., Bonfield, W., "A comparative study on the in vivo behavior of hydroxyapatite and silicon substituted hydroxyapatite granules," J Mater Sci Mater Med., 13(12), pp. 1199-1206 (2002).

[4] Landi, E., Celotti, G., Logroscino, G., Tampieri, A., "Carbonated hydroxyapatite as bone substitute," J Eur Ceram Soc., 23, pp. 2931-2937 (2003).

[5] Lusquinos, F., et al., "Calcium phosphate coatings obtained by Nd:YAG laser cladding: physicochemical and biologic properties," J Biomed Mater Res A., 64(4), pp. 630-637 (2003).

[6] Yuan, H., et al., "Osteoinduction by calcium phosphate biomaterials," J Mater Sci Mater Med., 9(12), pp. 723-726 (1998).

[7] Begley, C.T., Doherty M.J., Hankey, D.P., Wilson, D.J., "The culture of human osteoblasts upon bone graft substitutes," Bone, vol.14, pp. 661-666 (1993).

[8] Jokanovic`, V., Izvonar, D.,Dramic`anin, M.D., "Hydrothermal synthesis and nanostructure of carbonated calcium hydroxyapatite," J Mater Sci Mater Med., vol.17, pp. 539-546 (2006).

[9] Merry, J.C., et al., "Synthesis and characterization of carbonate hydroxyapatite," J Mater Sci Mater Med., 9(12), pp. 779-783 (1998).

[10] Webster, T.J., Ergun, C., Doremus, R.H., Siegel, R.W., Bizios, R., "Enhanced functions of osteoblasts on nanophase ceramics," Biomaterials, vol. 21, pp. 1803-1810 (2000).

[11] Krajewski, A., Mazzocchi, M., Buldini, P.L., Ravaglioli, A., Tinti, A., Taddei, P., Fagnano, C., 'Synthesis of carbonated hydroxyapatites: efficiency of the substitution and critical evaluation of analytical methods," J Mol Struct., vol.744, pp. 221-228 (2005).

[12] Gibson, I.R., Best, S.M., Bonfield W., "Chemical characterization of siliconsubstituted hydroxyapatite," J Biomed Mater Res., 44(4), pp. 422-428 (1998).

[13] Carlisle, E.M., "Silicon: A possible factor in bone calcification," Science, vol.167, pp. 179-280 (1970).

[14] Owen, M., "The origin of bone cells," Int Rev Cytol, vol.28, pp. 213-238 (1970).

[15] Olszta MJ, Cheng X, Jee SS, Kim Y, Kaufman MY, Douglas EP, Gower LB: "Bone structure and formation: A new perspective," Mater Sci Eng R Rep., vol. 58, pp. 77-116 (2007).

[16] Weiner, S., Wagner, H.D., "The material bone: structure mechanical function relations," Annual Review of Materials Science, vol. 28, pp. 271-298 (1998).

[17] Giraud-Guille, M.M., "Twisted liquid crystalline supramolecular arrangements in morphogenesis," Int. Rev.Cytol., vol. 166, pp.59-101(1996).

[18] Cowin, S.C., "Do liquid crystal-like flow processes occur in the supramolecular assembly of biological tissues," Non-Newronian Fluid Mechanics, vol.199, pp. 20 (2004).

[19]. Rodrigues, C.V.M., Serricella, P., Linhares, A.B.R., "Characterization of a bovine collagen-hydroxyapatite composite scaffold for bone tissue engineering", Biomaterials., 24(12), pp. 4987-4997 (2003).

[20] Doi, Y., Moriwaki,Y., Aoba, T., Okazaki, M., Takahashi, J., Joshin, K,. "Carbonate apatites from aqueous and non-aqueous media studied by ESR, IR, and X-ray diffraction: effect of NH4 ions on crystallographic parameters," J Dent Res, 61(2), pp. 429-434 (1982)

[21] Gower, L.B., Odom, D.J., "Deposition of calcium carbonate films by a polymerinduced liquid-precursor (PILP) process," J Cryst Growth, vol. 210, pp. 719-734 (2000).

[22] Bretaudiere, J.P., Spillman T., Methods of Enzymatic Analysis., Bergmeyer, Germany: Verlag Chemica. vol. 4, pp75-92, (1984).

[23] Wang, L., Zhao, G. Olivares-Navarrete, R., Bell, B.F., Wieland, M., Cochran, D.L., Schwartz, Z., Boyan, B.D., "Integrin beta1 silencing in osteoblasts alters substrate-dependent responses to 1,25-dihyroxy vitamin D3. Biomaterials," pp. 3716-3725 (2006).

[24] Featherstone, J.D.B., Pearson, S., LeGeros, R.Z., "An Infrared Method for Quantification of Carbonate in Carbonated Apatites," Caries Research, vol. 18, pp. 63-66 (1984).

CHAPTER 2

2.1 Introduction

The inorganic-organic biocomposite tissue known as bone is an intricate network of components that impart both high compressive strength and resistance to fracture. The specific and unique architecture of bone yields its mechanical properties and its surface chemistry imparts the proper environment for constant remodeling; the resorption of existing bone and formation new bone. During the formation of secondary bone, nanoscopic hydroxyapatite is aligned amongst self-assembled type I collagen fibrils. These collagen fibrils are in a parallel orientation within lamellae, which are arranged concentrically around blood vessels to form osteons. The fate of the osteons is to either exist as compact bone, being packed densely, or to form a trabecular network of microporous cancellous bone [1,2,3].

The biomineral naturally occurring in bone is a nano-crystalline carbonated hydroxylapatite inorganic, which comprises approximately 70% of the volume of this mineralized tissue [4,5]. Moreover, the carbonate content of bone is approximately 2-8wt%, depending upon the age of the individual [6,7]. Roughly, the remaining third component of this organ is an organic matrix, primarily consisting of collagen and small amounts of proteoglycan, lipid, and several noncollagenous proteins [3]. While bone cells, collagen fibers, various growth factors, and several noncollagenous proteins all contribute to the organic phase of bone, type I collagen is the paramount structural protein in bone's extracellular matrix and is the primary organic component of bone

[8,9,10]. Collagen assembles its tropocollagen units in a quarter-staggered array, which leads to hole and overlap zones that can be seen as periodic banding patterns. This quarter-stagger arrangement yields a regular array of 40 nm gaps within each periodic unit, and these are believed to be the locations where crystal nuclei are first observed in systems [11,12,13].

As a result, a major focus of biomaterials research has shifted towards preparation of synthetic carbonated hydroxyapatite (HA) bone substitutes that resemble the chemical composition and micro-architecture of bone [14]. During bone formation and remodeling, the osteoblast's nanoscopic and microscopic environment dictates its growth and differentiation [15,16,17,18]. In order to fully and functional mimic this physiological tissue, the surface chemical composition and mechanical integrity must be evaluated. In this present study, the surface topography and chemical composition is observed for both cortical and trabecular human bone of a 55 year old male patient. Topography and chemical composition is determined for mineralized, partially demineralized and fully demineralized bone. The degree of crystallinity is also evaluated for the aforementioned bone using X-Ray diffraction. The nanoscopic and microscopic surface roughness of these bone samples were additionally evaluated using AFM and profilometry, respectively. The wettability of this mineralized, partially and fully demineralized cortical and cancellous human bone was as well evaluated by determining the contact angle of water on these surfaces. Lastly, the elastic mechanical property of these aforementioned bone samples was evaluated by determining the elastic modulus of each sample.

2.2 Materials and Methods

2.2.1 Human Bone Wafer Preparation

Human bone wafers were provided and prepared by the Musculoskeletal Transplant Foundation. All tissue-processing procedures were performed in a non-sterile environment in either a fume hood or lab bench top. The donor tissues consisting of whole femurs and whole tibias were defrosted and all the adhering soft tissue and muscle were removed. A bandsaw was used to cut the condyles into 3mm cancellous sheets and all surrounding cortical tissue was removed. The cancellous sheets were cut to 2cm x 2cm square cancellous wafers. The femoral and tibial shafts were cleaned and cut down to 2cm rings. The semi-rings with flat sides were used to make 2cm by 2cm cortical wafers. A Sherline Mill was used to machine the thickness of the cortical wafers.

2.2.2 Mineralized Tissue Preparation

Cortical and cancellous tissue was cleaned with a combination of antibiotics, surfactant, and ethanol soaks followed by deionized water rinses. After the last deionized water soak the tissue was allowed to air dry. The cleaned tissue was packaged in plastic pouches and stored at -70°C until shipped. Bone wafers were oxygen plasma (PDC-32G Harrick Oxygen Plasma, Ithaca, NY) cleaned prior to experimentation to remove impurities that may have been absorbed to the surface upon opening the package.

2.2.3 Partially Demineralized Tissue Preparation

Cortical and cancellous tissue was cleaned as described in the mineralized tissue section. The demineralization process that was used was based on the methods employed by the Muscuskeletal Transplant Foundation to prepared demineralized bone grafts for clinical applications. After the deionized water soak, the tissue was then soaked in

hydrogen peroxide. In order to remove the hydrogen peroxide, the tissue was soaked in deionized water. After this water soak, the wafers were then soaked in hydrochloric acid and finally rinsed with deionized water. Lastly, the wafers were soaked in ethanol, then dried, packaged, and stored at -70°C until it was shipped. Bone wafers were oxygen plasma (PDC-32G Harrick Oxygen Plasma, Ithaca, NY) cleaned prior to experimentation to remove impurities that may have been adsorbed to the surface upon opening the package.

2.2.4 Fully Demineralized Tissue Preparation

Human bone wafers were initially soaked in hydrogen peroxide and rinsed with deionized water. Next, the bone wafers were soaked in ethanol and later dried. Following this, the wafers were soaked in hydrochloric acid and then rinsed with deionized water. Later the discs were soaked in sodium phosphate di-basic buffer to neutralize the tissue's pH. Finally, the wafers were rinsed and soaked with deionized water, then packaged in plastic pouches and stored at -70°C until shipped. Bone wafers were oxygen plasma (PDC-32G Harrick Oxygen Plasma, Ithaca, NY) cleaned prior to experimentation to remove impurities that may have been absorbed to the surface upon opening the package.

2.2.5 Statistical Analysis

For any given experiment, each data point represents the mean±standard error of six individual cultures. The following dataset descriptors were used to indicate the state of mineralization where, None = No demineralization, Partial= Partial demineralization, and Full= Full demineralization. Data were first analyzed by analysis of variance; when statistical differences were detected, Student's t-test for multiple comparisons using Bonferroni's modification was used. The following statistical markers represents

significant differences for the following: # [None vs. Partial], * [Partial vs. Full], and ·[Full vs. None]. p-Values <0.05 were considered to be significant.

2.3 Bone Wafer Characterizations

2.3.1 Scanning Electron Microscopy/Energy Dispersive X-ray Spectroscopy

All hydroxyapatite powder and discs were imaged using the LEO 1530 SEM (LEO Electron Microscope, Oberkochen, Germany). The wafers were sputter-coated with palladium-gold prior to scanning. All images were collected at a 4000x magnification. An 8kV EDS was used on uncoated samples to determine surface chemical composition of each bone wafer. Six different locations were evaluated using EDS. Calcium and phosphate peaks were selected for detection on the energy dispersive spectrum.

2.3.2 X-ray Diffraction

XRD was used in order to determine the degree of crystallinity of both the mineralized and demineralized wafers. The phase transitions of partially and fully demineralized bone wafers were analyzed using Cu *K*α1 radiation (λ=1.54056 A) at a scanning rate of 2 min -1. Two to three samples of each mineralization state of cortical and trabecular bone were analyzed to determine the crystallinity.

2.3.3 Profilometry

The surface roughness of both mineralized and demineralized cortical and trabecular bone wafers was determined using a mechanical stylus profiler KLA-Tencor Profilometer. R_A values were determined for all mineralized, partially and fully demineralized samples. Three different sections of each state of mineralization for cortical and trabecular bone were assessed.

2.3.4 Contact Angle

The wettability of each surface was evaluated by determining the angle at which water contacted its surface. The hydrophobic or hydrophilic nature of each surface was characterized using a KSV Instrument CAM 101. The fully demineralized trabecular bone did not maintain enough integrity to sustain the stress of testing, therefore no measurements were obtained.

2.3.5 Suface Elastic Modulus

Surface elastic modulus was determined by performing nanoindentation using a 130μm diameter spherical ruby tip on a MTS NanoIndenter. To simulate cell culture conditions samples were soaked in phosphate buffered saline (PBS) for 1 week and placed on a sample mount immersed in PBS-soaked absorbant foam to maintain hydration during indentation. Tip loads were incrementally applied at 0.5mN, 1mN, 2mN, 4mN, and 8mN, held for 30s, and subsequently unloaded. The displacement of the tip into the surface was recorded as a function of tip load. Using Hertzian theory for the contact of a sphere into an elastic half space, the model load vs. displacement curves were determined. To determine the elastic modulus based off the experimental load vs. displacement curves of the different copolymers, E values of the predicted curve were adjusted until the experimental data fit the predicted curve in the unloading region.

2.4 Results

Using scanning electron microscopy, we were able to observe surface variations of human mineralized and demineralized cortical and trabecular bone. The presence of calcium and phosphate was noticeably identified in the EDS spectrum and its continuous mineralized surface was reflected in the SEM image of this cortical bone (Figure 1a,d).

The absence of phosphate and calcium was likewise reflected in the partially demineralized cortical bone EDS spectrum, while the SEM image complimented the degree of mineralization (Figure 1b,e). The fully demineralized cortical bone EDS spectrum and SEM similarly represented the lack of calcium or phosphate mineralization (Figure 1c,f).

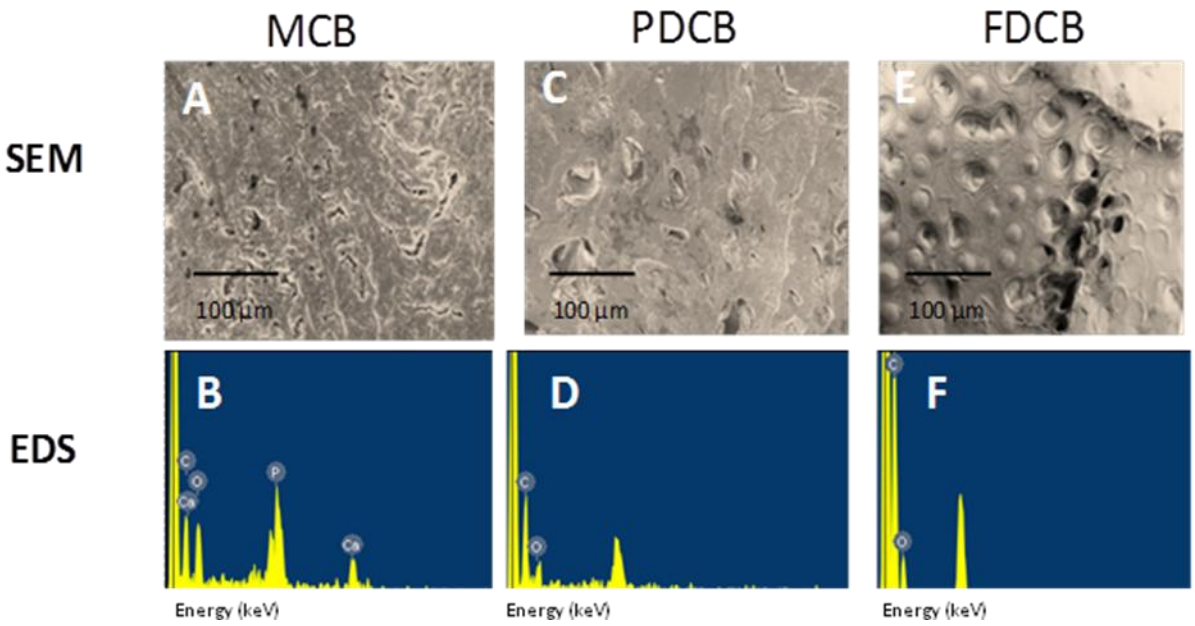

Figure 1. SEM of Cortical Bone. (A) Mineralized Cortical Bone (MCB) – 100kX; (B) EDS of MCB surface; (C) Partially Demineralized Cortical Bone (PDCB) – 100kX; (D) EDS of PDCB surface; (E) Fully Demineralized Cortical Bone (FDCB) – 100kX; (F) EDS of FDCB surface

When imaging trabecular bone, calcium's presence was clearly identified in the EDS spectrum and the spongy nature of this mineralized surface was observed in this SEM image (Figure 2a,d). The absence of phosphate and calcium was also reflected in the partially demineralized trabecular bone EDS spectrum, while the SEM image

additionally reflected the spongy character of this bone (Figure 2b,e). The fully demineralized trabecular bone EDS spectrum and SEM likewise represented the lack of calcium and phosphate mineralization (Figure 2c,f).

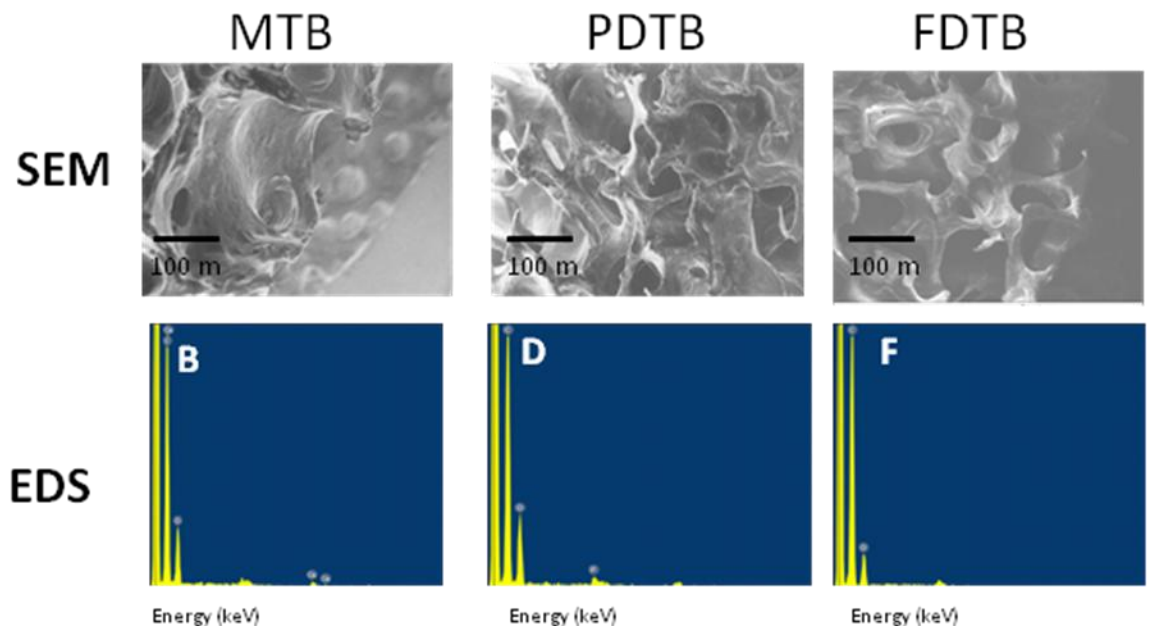

Figure 2. SEM of Trabecular Bone. (A) Mineralized Trabecular Bone (MTB) – 100kX ; (B) EDS of MTB surface (C) Partially Demineralized Trabecular Bone (PDTB) –100kX; (D) EDS of PDTB surface; (E) Fully Demineralized Trabecular Bone (FDTB) – 100kX; (F) EDS of FDTB surface

The crystallinity of both mineralized and demineralized cortical and trabecular human bone was accessed and determined in order to compare its structure to that of human bone in existing literature. The crystal X-ray diffraction pattern of the mineralized cortical bone exhibited the characteristic diffraction peaks at both 26° and 32° (Figure 3a). The diffraction pattern of the partially demineralized cortical bone displayed less crystalline characteristic peaks, whereas, the fully demineralized cortical bone reflected

the complete loss in these hydroxylapatite diffraction peaks and mineralization (Figure 3a).

Similarly, the crystal X-ray diffraction pattern of the mineralized trabecular bone exhibited the characteristic diffraction peaks at both 26° and 32° (Figure 3b). The diffraction pattern of the partially demineralized trabecular bone displayed similar characteristic peaks, although to a lesser degree crystallinity, while the fully demineralized trabecular bone did not exhibit these diffraction peaks and presented an overall loss of mineralization (Figure 3b).

A. X-ray Diffraction of Cortical Bone

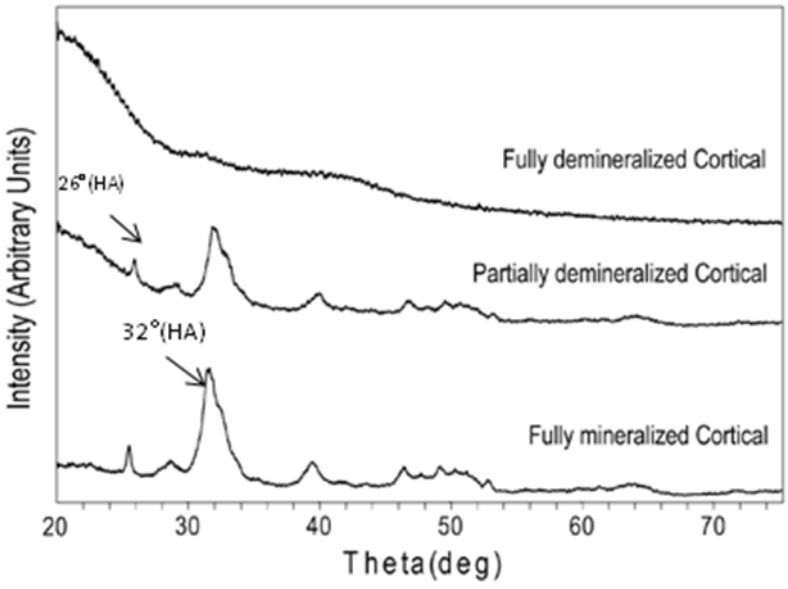

B. X-ray Diffraction of Trabecular Bone

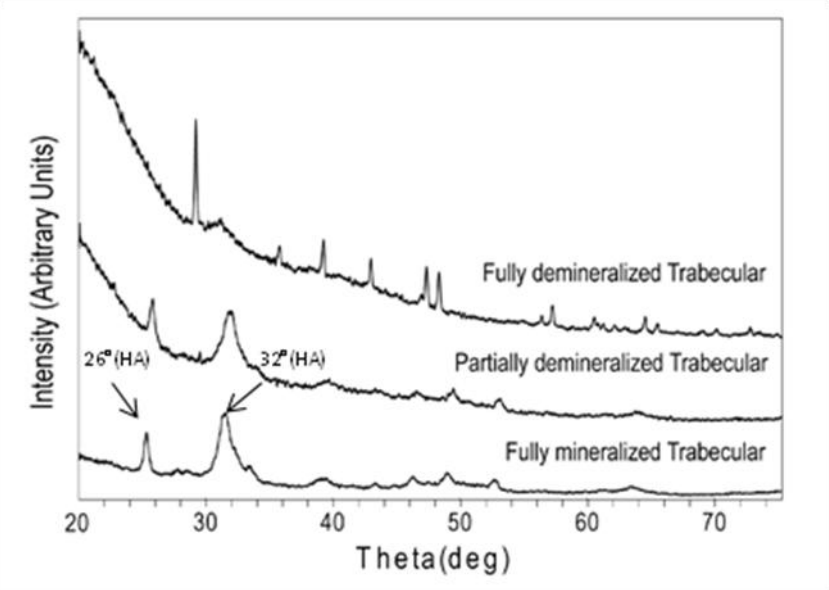

Figure 3. XRD of Cortical and Trabecular Bone. (A) X-ray Diffraction patterns of mineralized, partially and fully demineralized human cortical bone wafers using Cu *K*α1 radiation (λ=1.54056 A) at a scanning rate of 2 min -1. (B) X-ray Diffraction patterns of mineralized, partially and fully demineralized human trabecular bone wafers using Cu *K*α1 radiation (λ=1.54056 A) at a scanning rate of 2 min -1.

The surface roughness of mineralized and demineralized cortical bone was evaluated using both profilometry and AFM and varied dependent upon its prior physiologically connection to either the endosteum or periosteum tissue (Figure 4). Using a profilometry, with regard to trabecular bone, the surface roughness of both the mineralized and demineralized bone is significantly greater than that of the mineralized or demineralized cortical bone wafers (Figure 4a). Using AFM, a nano-scale surface roughness evaluation, mineralized cortical bone displayed the greatest surface roughness amongst all other osseous tissue, whether mineralized or demineralized (Figure 4b).

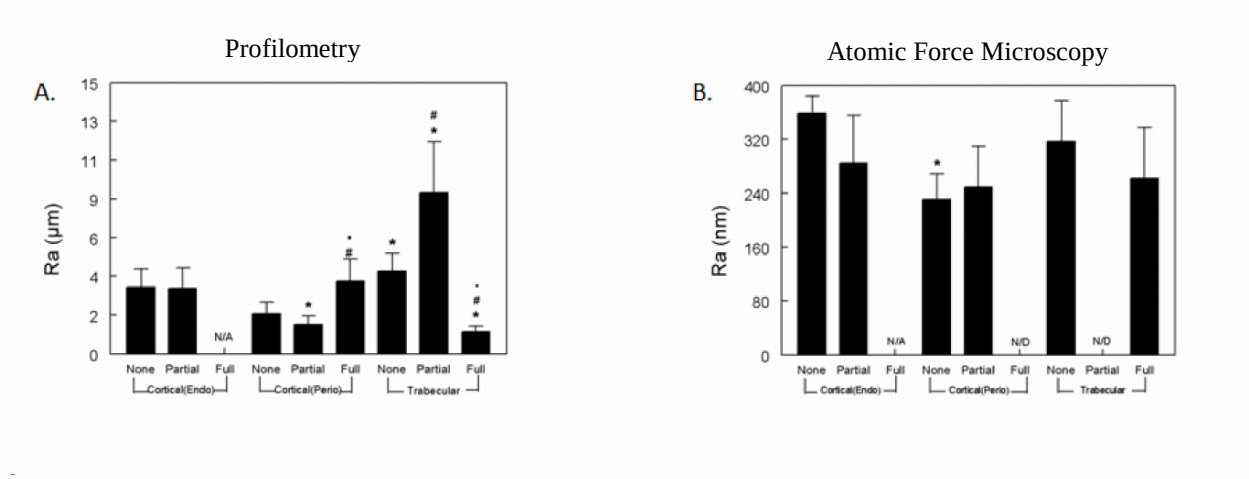

Figure 4. Profilometry and AFM of Cortical and Trabecular Bone. The micro-scale surface roughness of mineralized, partially and fully demineralized cortical and trabecular bone wafers was determined using (A) profilometry with a mechanical stylus profiler KLA- Tencor, and (B) nano-scale roughness was determined using a digitally scanning mechanical Atomic Force Microscope. (N/D = Not Detectable, N/A = Not Available)

When evaluating the contact angle of mineralized and demineralized cortical, all bone wafers presented a hydrophillic surface. Likewise, the fully demineralized trabecular human bone is also hydrophillic, with approximately a similar degree of wettability to that of the fully demineralized cortical bone previously attached to the periosteum (Figure 5a).

Nano-indentation was used to determine the stiffness of mineralized and demineralized cortical and trabecular bone. Mineralized cortical bone appears significantly stiffer than that of cortical demineralized bone, up to approximately four times as much. Mineralized and demineralized trabecular bone, on the other hand were comparable in stiffness to one another (Figure 5b).

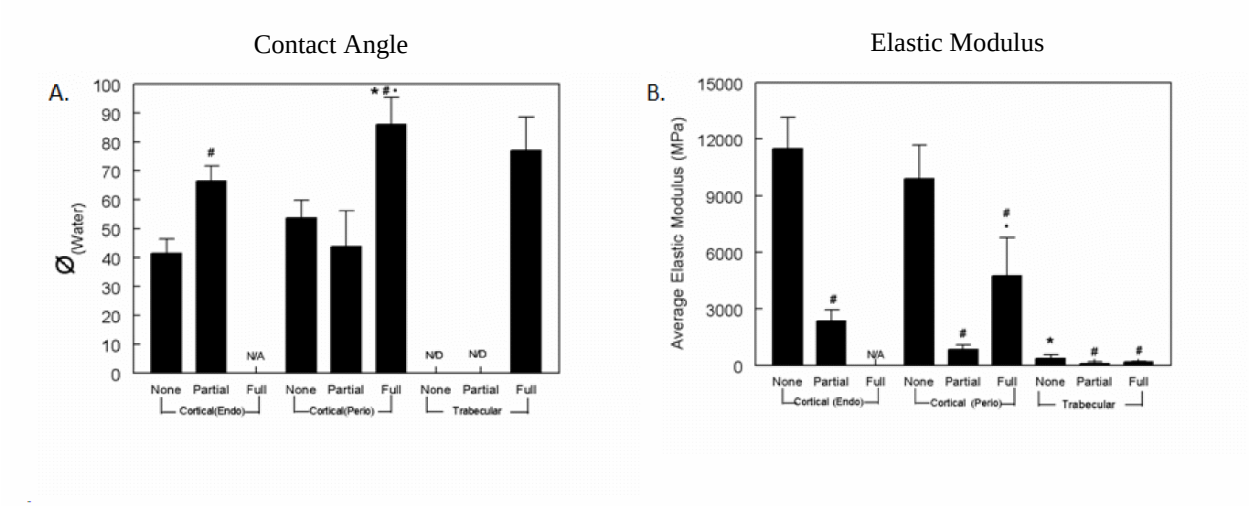

Figure 5. Contact Angle and Elastic Modulus of Cortical and Trabecular Bone. (A) Wettability of mineralized and demineralized cortical and trabecular human bone wafers using approximately one droplet of water in contact with surfaces evaluated using a KSV Instrument CAM 101 software. (N/D = Not Detectable, N/A = Not Available) and (B) surface elastic modulus of mineralized, partially and fully demineralized cortical and trabecular bone was determined by nanoindentation using a 130μm diameter spherical ruby tip on a MTS NanoIndenter. (N/D = Not Detectable, N/A = Not Available)

2.5 Discussion

Structural and chemical differences detected on bone wafer surfaces are directly related and imparted by the bone's state of mineralization. These structural and chemical attributes of mineralized, partially demineralized and fully demineralized cortical and trabecular bone dictate the osteo-surface environment and can be used as a templates for the design, processing and development of bone substitutes with varying degrees of osteoblast-likes characteristics. The surface elemental composition of the mineralized cortical bone quantifiably differed from that of the fully demineralized cortical bone wafers. However, several similarities between the mineralized and partially demineralized cortical bone wafers' chemical compositions reflect the significance of bone's mineralized state, more specifically, the absence or existence of mineral. The ablation of minerals on the bone's surface modulated the bone's crystallinity, surface

roughness, stiffness and hydrophobicity in a manner such that it was far less comparable to either the mineralized or partially demineralized states. Likewise, the similarity in crystallinity degree of both the cortical mineralized and partially demineralized bone was directly correlated to their nearly common degree of mineralization. This holds true for the varying degrees of mineralization of the trabecular bone as well. The surface chemistry of the mineralized and partially demineralized trabecular bone is attributed to their similar degree of mineralization, while the distinct differences in chemistry between the partially and fully demineralized bone were a function of their more distinct differences in states of mineralization.

The crystallinity of both the mineralized and partially demineralized trabecular bone was almost identical and yet the crystallinity of the mineralized and fully demineralized bone contrasted greatly, highlighting the significance of the mineralization state. The presence of mineral, whether to a greater or lesser extent, imparts consistent structural and chemical characteristics, whereas the ablation of mineral, which imparts a change in state of mineralization, more drastically alters bone surface dynamics and attributes. Moreover, the use of hydrogen peroxide and hydrochloric acid to demineralize the bone wafers as oppose to the more commonly used chelating agent, ethylenediaminetetraacetic acid (EDTA), may account for our results that are inconsistent with commonly accepted bone surface characterizations.

The ability of cells to adhere or anchor to the bone's surface is largely modulated by the bone's surface attributes, demonstrating a cell's dependence on chemical and structural characteristics when binding to a surface. A cell's surface interaction is thereby dictated by characteristics that are directly correlated and imparted by the bone's state of

mineralization. Fully characterizing the surface of cortical and trabecular bone is essential in establishing the framework for which bone biomaterials should be conceptualized and modeled. Varying degrees, as well as states of mineralization provides the necessary understanding of the integration and dependence amongst chemical and structural components of bone. With this comprehension, a more physiological and functional bone biocomposite can be formulated and designed.

2.6 References

[1] Freemont, A.J., "Basic bone cell biology," Int J Exp Pathol, 74(4), pp. 411-416 (1993).

[2] Huether, S.E., McCance, K.L., Understanding Pathophysiology. Second ed., St.Louis: Mosby (an imprint of Elsevier Science).

[3] Patel, N., Best, S.M., Bonfield, W., "A comparative study on the in vivo behavior of hydroxyapatite and silicon substituted hydroxyapatite granules," J Mater Sci Mater Med., 13(12), pp. 1199-1206 (2002).

[4] Landi, E., Celotti, G., Logroscino, G., Tampieri, A., "Carbonated hydroxyapatite as bone substitute," J Eur Ceram Soc., 23, pp. 2931-2937 (2003).

[5] Lusquinos, F., et al., "Calcium phosphate coatings obtained by Nd:YAG laser cladding: physicochemical and biologic properties," J Biomed Mater Res A., 64(4), pp. 630-637 (2003).

[6] Yuan, H., et al., "Osteoinduction by calcium phosphate biomaterials," J Mater Sci Mater Med., 9(12), pp. 723-726 (1998).

[7] Begley, C.T., Doherty M.J., Hankey, D.P., Wilson, D.J., "The culture of human osteoblasts upon bone graft substitutes," Bone, vol.14, pp. 661-666 (1993).

[8] Jokanovic`, V., Izvonar, D.,Dramic`anin, M.D., "Hydrothermal synthesis and nanostructure of carbonated calcium hydroxyapatite," J Mater Sci Mater Med., vol.17, pp. 539-546 (2006).

[9] Merry, J.C., et al., "Synthesis and characterization of carbonate hydroxyapatite," J Mater Sci Mater Med., 9(12), pp. 779-783 (1998).

[10] Webster, T.J., Ergun, C., Doremus, R.H., Siegel, R.W., Bizios, R., "Enhanced functions of osteoblasts on nanophase ceramics," Biomaterials, vol. 21, pp. 1803-1810 (2000).

[11] Krajewski, A., Mazzocchi, M., Buldini, P.L., Ravaglioli, A., Tinti, A., Taddei, P., Fagnano, C., 'Synthesis of carbonated hydroxyapatites: efficiency of the substitution and critical evaluation of analytical methods," J Mol Struct., vol.744, pp. 221-228 (2005).

[12] Gibson, I.R., Best, S.M., Bonfield W., "Chemical characterization of siliconsubstituted hydroxyapatite," J Biomed Mater Res., 44(4), pp. 422-428 (1998).

[13] Carlisle, E.M., "Silicon: A possible factor in bone calcification," Science, vol.167, pp. 179-280 (1970).

[14] Owen, M., "The origin of bone cells," Int Rev Cytol, vol.28, pp. 213-238 (1970).

[15] Olszta MJ, Cheng X, Jee SS, Kim Y, Kaufman MY, Douglas EP, Gower LB: "Bone structure and formation: A new perspective," Mater Sci Eng R Rep., vol. 58, pp. 77-116 (2007).

[16] Weiner, S., Wagner, H.D., "The material bone: structure mechanical function relations," Annual Review of Materials Science, vol. 28, pp. 271-298 (1998).

[17] Giraud-Guille, M.M., "Twisted liquid crystalline supramolecular arrangements in morphogenesis," Int. Rev.Cytol., vol. 166, pp.59-101(1996).

[18] Cowin, S.C., "Do liquid crystal-like flow processes occur in the supramolecular assembly of biological tissues," Non-Newronian Fluid Mechanics, vol.199, pp. 20 (2004).

[19]. Rodrigues, C.V.M., Serricella, P., Linhares, A.B.R., "Characterization of a bovine collagen-hydroxyapatite composite scaffold for bone tissue engineering", Biomaterials., 24(12), pp. 4987-4997 (2003).

[20] Doi, Y., Moriwaki,Y., Aoba, T., Okazaki, M., Takahashi, J., Joshin, K,. "Carbonate apatites from aqueous and non-aqueous media studied by ESR, IR, and X-ray diffraction: effect of NH4 ions on crystallographic parameters," J Dent Res, 61(2), pp. 429-434 (1982)

[21] Gower, L.B., Odom, D.J., "Deposition of calcium carbonate films by a polymerinduced liquid-precursor (PILP) process," J Cryst Growth, vol. 210, pp. 719-734 (2000).

[22] Bretaudiere, J.P., Spillman T., Methods of Enzymatic Analysis., Bergmeyer, Germany: Verlag Chemica. vol. 4, pp75-92, (1984).

[23] Wang, L., Zhao, G. Olivares-Navarrete, R., Bell, B.F., Wieland, M., Cochran, D.L., Schwartz, Z., Boyan, B.D., "Integrin beta1 silencing in osteoblasts alters substrate-dependent responses to 1,25-dihyroxy vitamin D3. Biomaterials," pp. 3716-3725 (2006).

[24] Featherstone, J.D.B., Pearson, S., LeGeros, R.Z., "An Infrared Method for Quantification of Carbonate in Carbonated Apatites," Caries Research, vol. 18, pp. 63-66 (1984).

[25] Olszta M.J., Cheng X., Jee S.S., Kim Y., Kaufman M.Y., Douglas E.P., Gower L.B., "Bone structure and formation: A new perspective," Mater Sci Eng R Rep., vol. 58, pp. 77-116 (2007).

CHAPTER 3

3.1 Introduction

Traumatic bone injuries causing segmental defects and diseases that lead to the deterioration of bone are the primary catalysts dictating a continuous need for readily available bone graft substitutes. Autologous bone is by far the most effective bone graft material owing to its intrinsic osteogenic properties [1]. However, donor site morbidity and limited availability, especially in adolescents, present serious challenges when using autologous bone, and thus drives the demand for the development of alternative graft materials and substitutes.

To date, several materials have been evaluated to determine their biocompatibility and success as potential bone graft substitutes. Synthetic bioactive glass, ceramics, coral, and calcium phosphate powders are but only a few of those assessed [2]. Synthetic hydroxyapatite, $Ca_{10}(PO_4)_6(OH)_2$, closely resembles the chemistry of the mineral component of bone, however the biomineral naturally occurring in bone is a nano-crystalline carbonated apatite [3]. Moreover, the carbonate content of bone varies with the age of the individual, approximately 2-8 wt% [3], further adding complexity in determining the biological effects of the carbonate containing mineral. While research has shifted toward development of synthetic carbonated hydroxyapatite (HA) bone substitutes that resemble the chemical composition and micro-architecture of bone [4], relatively little is known about how the incorporated carbonate affects bone cells.

Synthetic carbonated apatite is often produced by incorporating carbonate ions into the hydroxyapatite lattice structure, replacing either the hydroxyl groups or phosphate ions [6]. Replacing the hydroxyl group gives rise to a type-A substitution,

while replacement of the phosphate group yields type-B carbonation. Type-B carbonate in the apatite lattice has previously been shown to cause a decrease in crystallinity and an increase in solubility in both *in vitro* and *in vivo* studies. Type-A carbonate substitution yields a lower affinity for human trabecular osteoblasts when compared to HA, demonstrated by lower cell attachment and collagen production [7]. A-B type carbonation is the state of physiological carbonated hydroxyapatite and can be achieved by substituting carbonate ions into both the phosphate and hydroxyl groups [8].

In the present study, we characterized three different carbonated hydroxyapatite substrates and investigated their effects on osteoblast differentiation. Carbonate ions were incorporated into the hydroxyapatite powders. The phosphate and hydroxyl groups were reduced as shown by chemical analysis of the substrate surfaces. The carbonated hydroxyapatites with increasing carbonate concentrations were molded, pressed, and fired into 14mm discs; surface chemical compositions and micro-architecture were characterized. In order to determine effects on cell number and differentiation, human osteoblast-like MG63 cells were cultured on each surface and differentiation markers as well as local growth factors were evaluated.

3.2 Materials and Methods

3.2.1 HA Disc Design and Preparation

Stoichiometric pure hydroxyapatite and carbonated hydroxyapatite powders were used in this study. The pure hydroxyapatite powder was prepared by an aqueous precipitation reaction between a calcium nitrate solution and a diammonium hydrogen phosphate $(NH_4)_2HPO_4$ solution. The carbonated hydroxyapatite powders were prepared by an aqueous precipitation reaction between a calcium nitrate solution, diammonium

hydrogen phosphate $(NH_4)_2HPO_4$ solution, and three different concentrations of ammonium carbonate (3.88, 4.85 and 5.82 weight percents), designated C1, C2, and C3, respectively. The reaction temperature was maintained at 60°C and the pH at 11. The settled precipitate was aged for 1 hour at 60°C. After aging, the white precipitate was left overnight and then decanted, centrifuged, and washed with distilled water until the ammonia and all residual free calcium salts were removed. Each of the above prepared precipitates were dried at 80°C and then grinded.

The pure and substituted hydroxyapatite powders containing carbonate with varying ion concentrations were pressed into 17mm discs using a press and die and fired to ensure compactness. During the firing process, the discs shrank approximately 18%, which was accounted for in order to produce approximately 14mm discs for cell culture. One gram of each powder was used to press an individual disc and 500 µls of polyvinyl alcohol (PVA) was used as a binder to coalesce the powder. These discs were preheated to 200°C prior to firing to prevent charring and cracking. After pre-heating, the discs were then sintered to improve their compactness and integrity, an approach used to ensure the discs remained intact during cell culture. The discs were fired using a controlled temperature schedule that heated the discs from room temperature to 500°C at an initial 5°C/min rate up to 200°C, and then at a 1°C/min rate until the final temperature was reached. The discs were cooled similarly at a 1°C/min rate in order to prevent charring and cracking and to ensure the removal of the PVA binder.

3.2.2 Sterilization of Discs

The discs were soaked and washed twice for 3 hours in 50mM ammonium bicarbonate prior to sterilization. After drying the discs in a conventional oven heated to

100°C, both sides of the discs were sterilized using an oxygen plasma cleaner (PDC-32G Harrick Oxygen Plasma, Ithaca, NY). Discs were then placed in sterile non-tissue culture treated polystyrene plates for use in the following cell culture studies described below. The cells were then soaked in the culture media containing Dulbecco's modified Eagle medium (DMEM) containing 10% fetal bovine serum (FBS) and 1% penicillin/streptomycin for 24 hours prior to cell culture to prepare the surfaces for cell seeding.

3.2.3 Characterization of Carbonated Hydroxyapatite Discs

All hydroxyapatite powder and discs were imaged using the LEO 1530 SEM (LEO Electron Microscope, Oberkochen, Germany). Discs were sputter-coated with palladium-gold prior to scanning. All images were collected at a 4000x magnification using an 8kV laser. EDS was assessed on uncoated samples to determine surface chemical composition of each carbonated apatite. XRD was conducted on both powder and pressed samples while being heated in order to determine the approximate temperature at which phase transition of hydroxyapatite powder may occur. For C1, C2, and C3 discs, decomposition of hydroxyapatite into $CaCO_3$ began to occur around 700 to 750°C. The potential phase transitions and crystallinity of C1, C2, and C3 were analyzed using Cu $K_{\alpha 1}$ radiation (λ=1.54056 A) at a scanning rate of 2 min^{-1}.

The surface roughness of the fired hydroxyapatite discs was determined using a mechanical stylus profiler KLA-Tencor Profilometer. R_A values were determined by scanning three different sections of the surfaces for the C1, C2, and C3 experimental discs however the sides of the surfaces were not assessed. The wettability of each surface was evaluated by determining the angle at which water contacted its surface. A droplet of

water, approximately 500 µls, was dispensed on the surface of each type of mineralized disc. Two different discs for each state of mineralization were evaluated. The hydrophobic or hydrophilic nature of each surface was characterized using KSV Instrument CAM 101 software.

3.2.4 Cell Culture

Human osteoblast-like MG63 cells were obtained from the American Type Culture Collection (Rockville, MD). Cells cultured on tissue culture treated polystyrene (TCPS) were compared to those on the pure and carbonated HA substitutes in non-tissue culture treated wells. The cells were cultured in Dulbecco's modified Eagle medium (DMEM) containing 10% fetal bovine serum (FBS) and 1% penicillin/streptomycin at 37°C in an atmosphere of 5% CO_2 and 100% humidity. Non-tissue culture treated plates were used in order to discourage cell attachment to the walls of the wells allowing all growth factors evaluated in conditioned media to be produced exclusively from cells attached to the surface of the discs. MG63 cells were added to the 24 well plates at a cell seeding density of 20,000/cm^2 in 500µl of medium per well. Wells containing the control MG63 cells plated on the TCPS were used as a measure of the cells reaching confluence. Media were changed at 72 hr intervals until cells reached confluence, at which time the cells in all cultures were harvested.

3.2.5 Cell Response

Cell number was determined in all cultures 24 h after cells on TCPS reached confluence. Cells were released from the surfaces by two sequential incubations in 0.25% trypsin for 10 min at 37°C, in order to ensure that any remaining cells were removed

from the HA surfaces. Released cells were counted using an automatic cell counter (Z1 cell and particle counter, Beckman Coulter, Fullerton, CA).

We used two determinants of osteoblast differentiation: alkaline phosphatase-specific activity (orthophosphoric monoester phosphohydrolase, alkaline; E.C. 3.1.3.1) of cell lysates, and osteocalcin content of the conditioned media. Alkaline phosphatase is an early marker of differentiation and reaches its highest level as mineralization is initiated. Osteocalcin is a late marker of differentiation and increases as mineral is deposited. Cell lysates were collected by centrifuging the cells after counting. Enzyme activity was assayed by measuring the release of p-nitrophenol from p-nitrophenylphosphate at pH 10.2 and results were normalized to protein content of the cell lysates [10]. The levels of osteocalcin in the conditioned media were measured using a commercially available radioimmunoassay kit (Human Osteocalcin RIA Kit, Biomedical Technologies, Stoughton, MA) and normalized to cell number.

The conditioned media were also assayed for growth factors and cytokines. Osteoprotegerin (OPG) was measured using an enzyme-linked immunosorbent (ELISA) kit (DY805 Osteoprotegerin DuoSet, R&D System, Minneapolis, MN). Vascular endothelial growth factor levels were also measured using an enzyme-linked immunosorbent (ELISA) kit (DY233 VEGF DuoSet, R&D System, Minneapolis, MN).

3.2.6 Statistical Analysis

The data presented are from one of two separate sets of experiments. Both sets of experiments yielded comparable observations. For any given experiment, each data point represents the mean±standard error of six individual cultures. Data were first analyzed by

analysis of variance; when statistical differences were detected, Student's t-test for multiple comparisons using Bonferroni's modification was used. For the surface characterizations and cell response results, * represents [Cn vs. HA], + represents [C3 vs. C2], and $ represents [C3 vs. C1] where 0% carbonate represents the pure HA control. p-Values<0.05 were considered to be significant.

3.3 Results

Scanning electron microscopy was able to detect slight variations in the surface features of the HA and CO_3^{2}-HA surfaces (Figure 6). SEM imaging showed that the C1, C2, and C3 surfaces appeared more granular and rougher with increasing carbonate content.

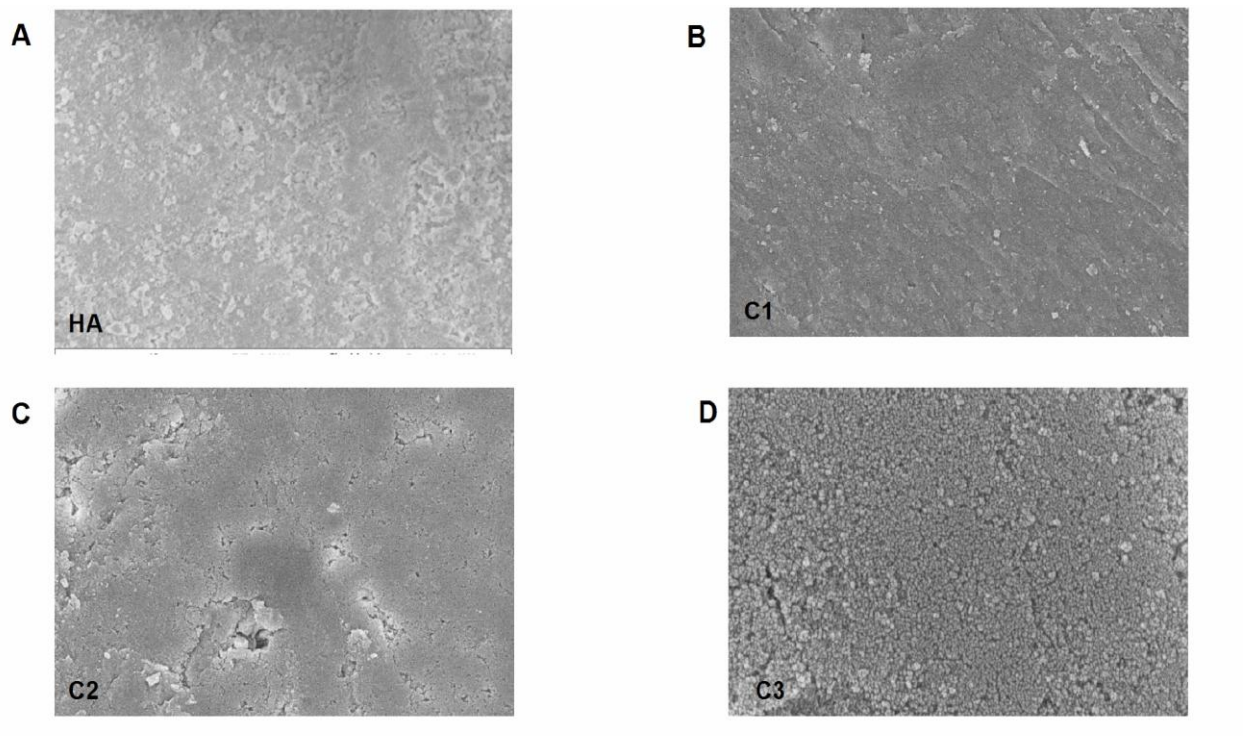

Figure 6. SEM of HA and CO_3^{2-}HA. Fired HA and CO_3^{2-}HA powders were coated with gold and their surfaces were imaged at 4000 X using an 8 kV power source: (A) HA, (B) C1 (3.8% CO_3^{2-}HA), (C) C2 (4.8% CO_3^{2-}HA), (D) C3 (5.8% CO_3^{2-}HA).

The surface chemistry differed as well. The carbon content exposed to the cells on the surface of the CO_3^{2}-HA substitutes was significantly greater than that of the pure HA substitute, and increased monotonically for each CO_3^{2}-HA substitute. The Ca/P of the pure synthetic hydroxyapatite produced in the present study was 1.77, which is within the typical range of synthetic HA (1.5 – 2.0) (3).

A-B type carbonated hydroxyapatite substitutes have carbonate ions replacing both the hydroxyl and phosphate groups of HA. Each substitute was sintered to 500°C in order to produce intact and compact discs. In order to determine the appropriate firing temperature, each CO_3^{2}-HA powdered substitute was heated to 1000°C. At approximately 700°C, CO_3^{2}-HA substitutes began to dissociate into calcium oxide and tri-calcium phosphate by-products. XRD confirmed that the crystallinity of each CO_3^{2}-HA substitute retained the hydroxyapatite structure and nature (Figure 7). The crystal X-ray diffraction patterns of HA, C1, C2 and C3 were comparable to that of standard stoichiometric synthetic HA. Increasing the carbonate content, however, resulted in the appearance of peaks corresponding to calcium carbonate for the C3 formulation.

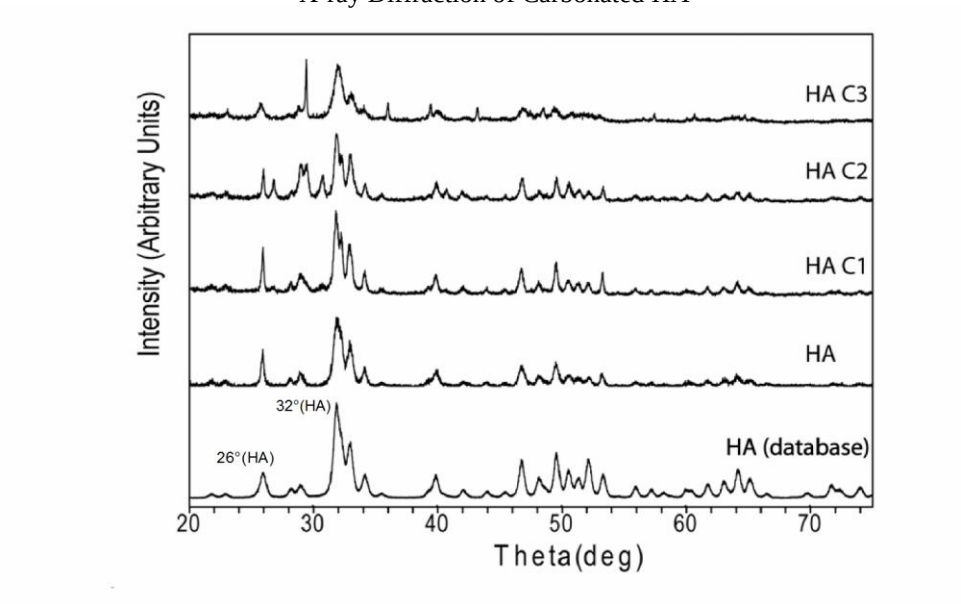

Figure 7. XRD analysis of CO_3^{2-}HA discs. The phase of the fired CO_3^{2-}HA discs was analyzed using Cu $K_{\alpha 1}$ radiation (λ=1.54056 A) at a scanning rate of 2 min^{-1}. The phase of the fired CO_3^{2-}HA is compared to the standard phase of hydroxyapatite.

Surface roughness of C3 was almost 2.5 times greater than that of the pure hydroxyapatite, and approximately 4 times greater than that of C2 (Figure 8a). HA surface roughness was greater than that of either C1 or C2. All CO_3^{2}-HA substitutes were found to be relatively hydrophilic, having a contact angle less than 90°C (Figure 8b). However, C3 had the highest contact angle and nearly approached the threshold for hydrophobicity. It was also determined that the wettability of all CO_3^{2}-HA formulations decreased with increasing carbonate content.

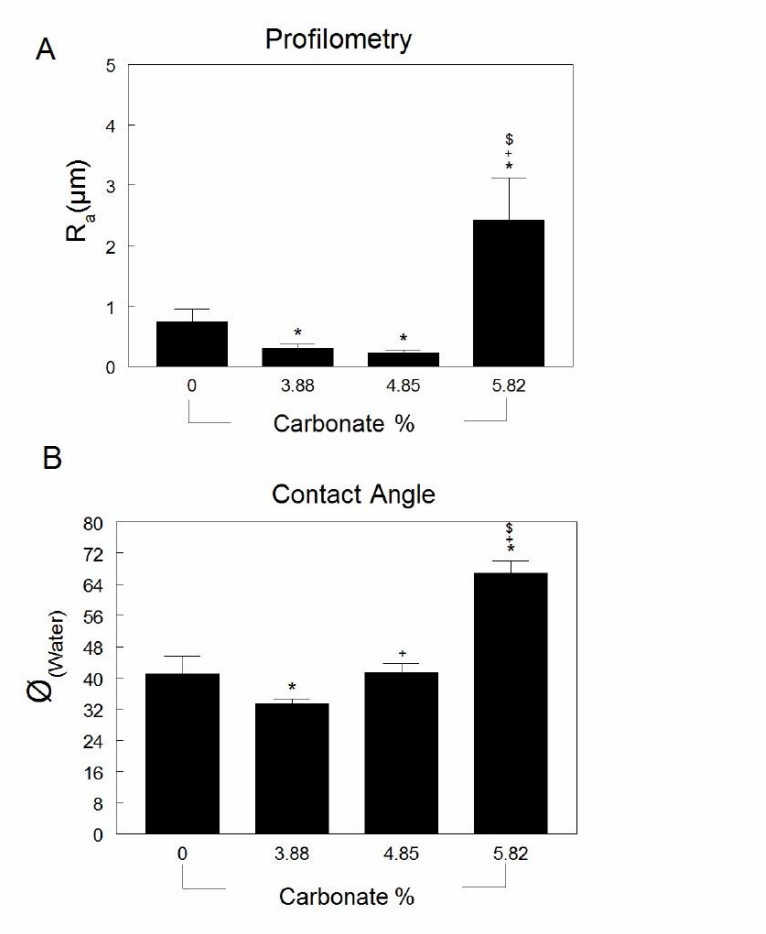

Figure 8. Surface roughness and wettability of HA and CO_3^{2-}HA discs. (A) R_A values were determined for pure HA and CO_3^{2-}HA substitutes. (B) Contact angles of pure HA and CO_3^{2-}HA substitutes. Values are mean±SEM per variable with n=6. Data were analyzed by ANOVA and significant differences between groups determined using the Bonferroni modification of Student's *t*-test.

Cell number on the CO_3^{2-}HA substrates increased with increasing carbonate concentration. The number of cells observed on C3 surfaces was approximately twice the amount on C1 surfaces (Figure 9a). HA discs without CO_3^{2} surfaces supported the least amount of cells.

Overall differentiation of MG63 osteoblast-like cells decreased with increasing carbonate content of the surfaces. Alkaline phosphastase specific activity was reduced in

a dose-dependent manner as function of carbonate content (Figure 9b). Osteocalcin also decreased with increasing carbonate concentration, with cells on C3 surfaces producing the lowest levels (Figure 9c).

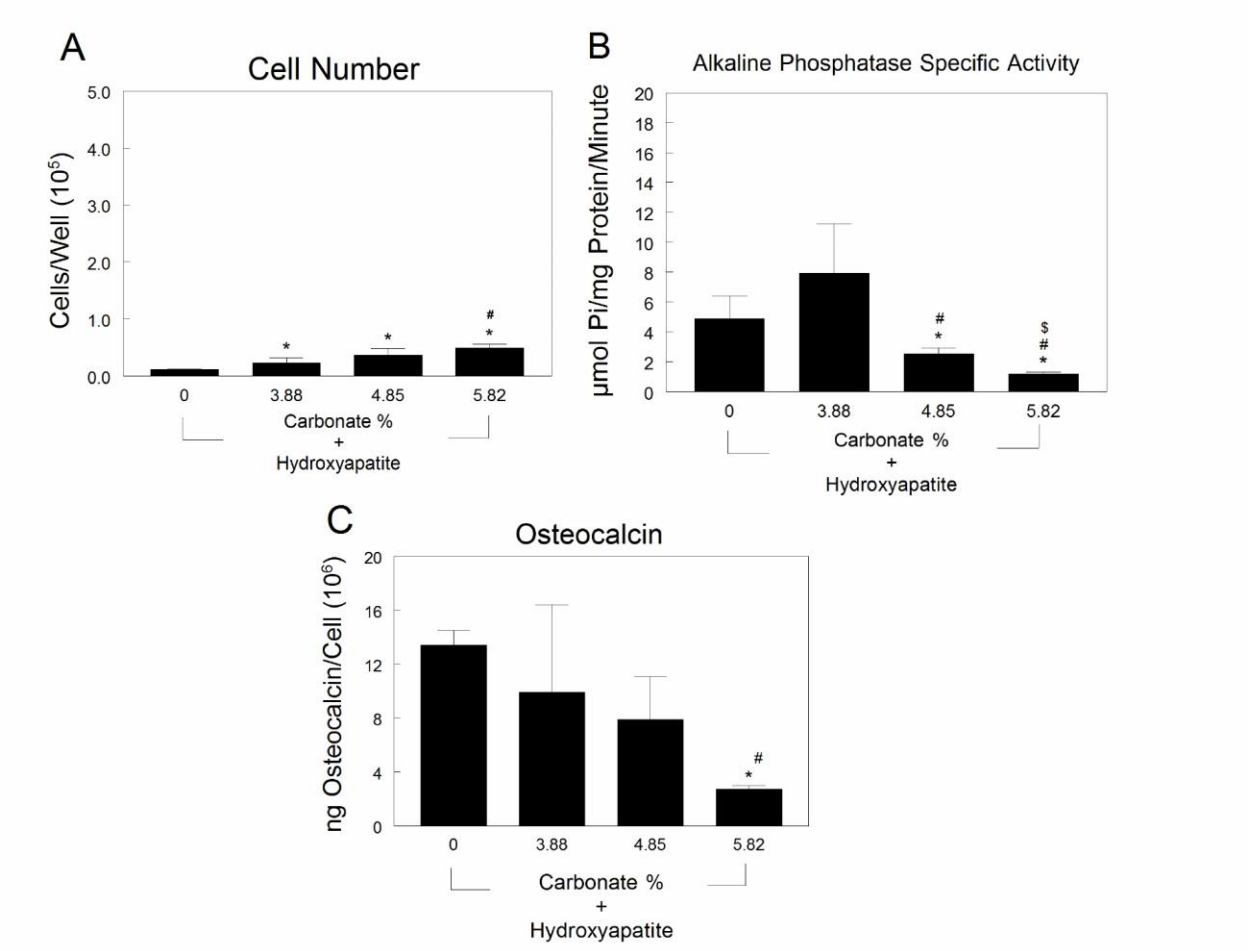

Figure 9. Responses of MG63 cells cultured on HA and CO_3^{2-}HA discs. (A) Cell number was measured 24 hrs after cells reached confluence on surfaces. (B) Alkaline phosphatase-specific activity was measured in harvested cells and (C) osteocalcin levels were measured in conditioned media of confluent cultures. Values are mean±SEM of six independent cultures. Data are from one of three separate experiments, with comparable results. Data were analyzed by ANOVA and significant differences between groups determined using the Bonferroni modification of Student's *t*-test.

Osteoprotegerin (OPG) levels were reduced by 70% when carbonate was present compared to pure HA (Figure 10a). The effect was not concentration dependent. Similarly, VEGF-A levels were decreased by carbonate compared to HA (Figure 10b). The effect was greatest at the lowest carbonate concentration (80% reduction). At higher carbonate concentrations the effect was less pronounced.

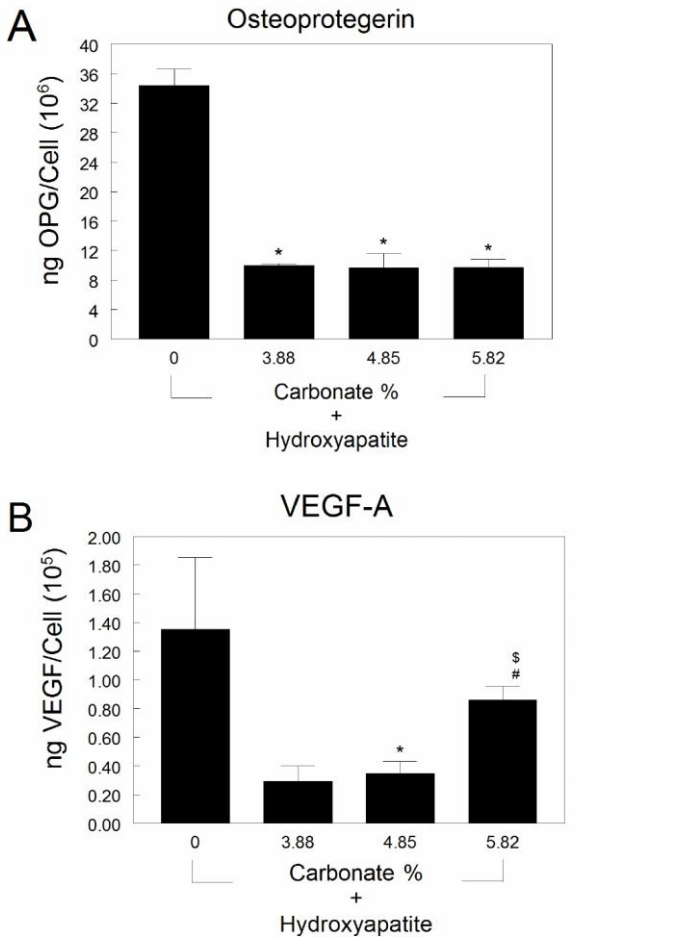

Figure 10. Effect of HA and CO_3^{2-}HA discs on MG63 cell production of OPG and VEGF-A. OPG (A) and VEGF-A (B) were measured in the conditioned media of confluent cultures. Data are from one of three separate experiments, with comparable results. Data were analyzed by ANOVA and significant differences between groups determined using the Bonferroni modification of Student's *t*-test.

3.4 Discussion

This study has shown that nanocrystalline powders containing CO_3^{2-} can be used to generate carbonate substituted HA discs that support MG63 cell attachment, growth, and expression of proteins associated with differentiated osteoblasts. The surfaces of the discs differ structurally and chemically depending upon the original carbonate content of the nanopowders. Importantly, cell response is sensitive to these differences.

Surface analysis demonstrated that the calcium phosphate ratio of the synthetic HA was comparable to the theoretical 1.67 ratio of pure hydroxyapatite. The calcium phosphate ratios of C1, C2, and C3 monotonically increased as a result of increased carbonate close to that of biological apatite [11]. At the highest concentration of CO_3^{2-}, calcium phosphate ratio was greater than 2 on the surface suggesting that the HA may have been less crystalline. Even after firing, the C1, C2, and C3 surfaces maintained a carbonate weight percent within the 2-8 wt% physiological range for biomineral [3]. As expected, CO_3^{2-} content on the surface was highest on the C3 surface, which correlated with the higher contact angle that was observed. The marked increase in contact angle might also have resulted in the increased roughness seen on the C3 surface.

Interestingly, the C3 surface supported the highest number of cells but the cells growing on the C3 surface had the lowest alkaline phosphatase activity and osteocalcin product. This suggests that cells on the C3 surface were less differentiated than the cells on the other substrates. We have shown that TiO_2 and Ti6Al4V surfaces with Ra's comparable to the 3μm Ra of the C3 surface support greater osteoblastic differentiation than smoother substrates, particularly when the surface is hydrophilic [12, 13, 14]. Thus

the reduced differentiation of MG63 cells on C3 was likely due to the chemistry of the surface, and was not dictated by the surface roughness alone.

These observations collectively suggest that an optimal carbonate concentration will depend on the desired biological outcome. The C3 surface supported the greatest production of VEGF-A, which is an angiogenic factor needed to promote revascularization of a wound site. By tailoring the carbonate content as well as the surface roughness, the osteogenic and angiogenic properties of a bone graft material may be achieved. Altogether, these results indicate that the overarching variable dictating cellular response to carbonated hydroxyapatite bioceramic appears to be the surface chemistry, which in this study was modulated by ionic substitutions, while the surface roughness also likely plays an important role. This suggests that modification of the chemical composition of a calcium phosphate biomaterial has the potential to enhance or ablate osteoblast-like cell growth and differentiation.

Bone biomaterials consisting of approximately 70% biomineral and 30% organic tissue, which thereby mimic the necessary chemical composition of bone, will likely provide functional replacements for compromised osseous tissue and segmental defects. Identifying the appropriate concentration of carbonate to incorporate into the hydroxyapatite substate is essential to creating the most functional representative of physiological bone. Controlling the surface chemistry of biomaterials during their formation will likely encourage bone ingrowth and integration of an implant material in the absence of autologous bone.

Normal bone mineral is a carbonated-apatite, but there are limited data on the effect of mineral containing carbonate on cell response. We characterized surface chemical compositions of three experimental carbonated hydroxyapatite (CO_3^{2}-HA) substrates and investigated their effect on osteoblast differentiation. Carbonate ions were incorporated into the hydroxyapatite powder to create CO_3^{2}- HA powders with increasing carbonate concentrations designated as C1 (3.88%), C2 (4.85%), and C3 (5.82%). The carbonated HA powder was molded, pressed, and fired into 14mm discs. We observed that calcium phosphate ratios increased monotonically with increasing carbonate content, whereas differentiation of MG63 cells decreased. CO_3^{2}-HA surfaces also affected factor production. Addition of carbonate caused a 70% reduction in osteoprotegerin (OPG) compared to cultures on pure HA, but the effect of carbonate was not dose-dependent. Low carbonate content reduced VEGF-A by 80%, but higher levels of carbonate reversed this effect in a concentration dependent manner, with the C3 VEFG-A levels approximately twice that of C1 levels. These observations collectively indicate that bone cells are sensitive to carbonate content in bone mineral and the effects of carbonate substitution vary with the outcome being measured. Overall, this study provides a preliminary understanding of how carbonate substitution within hydroxyapatite modulates cellular behavior.

3.5 References

[1] Patel N, Best S, Bonfield W. A comparative study on the in vivo behavior of hydroxyapatite and silicon substituted hydroxyapatite granules. J Mater Sci Mater Med. 13(12), pp.1199-1206 (2002).

[2] Landi, E., Celotti, G., Logroscino, G., Tampieri, A., "Carbonated hydroxyapatite as bone substitute," J Eur Ceram Soc., 23, pp. 2931-2937 (2003).

[3] Yuan, H., Yang, Z., Li, Y., Zhang, X., De Bruijn, J.D., De Groot, K., "Osteoinduction by calcium phosphate biomaterials," J Mater Sci Mater Med., 9(12), pp. 723-726 (1998).

[4] Sun, L., Chow, L.C., Frukhtbeyn, S.A., Bonevich, J.E., "Preparation and properties of nanoparticles of calcium phosphates with various Ca/P ratios," J Res Natl Inst Stand Technol., 115(4), pp. 243-255 (2010).

[5] Begley, C.T., Doherty M.J., Hankey, D.P., Wilson, D.J., "The culture of human osteoblasts upon bone graft substitutes," Bone, vol.14, pp. 661-666 (1993).

[6] Lusquinos, F., De Carlos, A., Pou, J., Arias, J.L., Boutinguiza, M., León, B., Pérez-Amor, M., Driessens, F.C., Hing, K., Gibson, I., Best, S., Bonfield, W., "Calcium phosphate coatings obtained by Nd:YAG laser cladding: physicochemical and biologic properties," J Biomed Mater Res A., 64(4), pp. 630-637 (2003).

[7] Webster, T.J., Ergun, C., Doremus, R.H., Siegel, R.W., Bizios, R., "Enhanced functions of osteoblasts on nanophase ceramics," Biomaterials, vol. 21, pp. 1803-1810 (2000).

[8] Krajewski, A., Mazzocchi, M., Buldini, P.L., Ravaglioli, A., Tinti, A., Taddei, P., Fagnano, C., 'Synthesis of carbonated hydroxyapatites: efficiency of the substitution and critical evaluation of analytical methods," J Mol Struct., vol.744, pp. 221-228 (2005).

[9] Gibson, I.R., Best, S.M., Bonfield W., "Chemical characterization of siliconsubstituted hydroxyapatite," J Biomed Mater Res., 44(4), pp. 422-428 (1998).

[10] Bretaudiere, J.P., Spillman T., Methods of Enzymatic Analysis., Bergmeyer, Germany: Verlag Chemica. vol. 4, pp75-92, (1984).

[11] Mostafa, A.A., Oudadesse, H., Mohamed, M.B., Foad, E.S., Le Gal, Y., "Convenient approach of nanohydroxyapatite polymeric matrix composite," Chem. Eng. J., vol. 136, pp. 187-192 (2009).

[12] Olivares-Navarrete, R., Hyzy, S.L., Gittens, R.A., Schneider, J.M., Haithcock, D.A., Ullrich, P.F., Slosar, P.J., Schwartz, Z., Boyan, B.D., "Rough titanium alloys regulate osteoblast production of angiogenic factors," Spine J.. doi:pii: S1529-9430(13)00399-9. 10.1016/j.spinee.2013.03.047 (2013)

[14] Gittens, R.A., Olivares-Navarrete, R., Cheng, A., Anderson, D.M., McLachlan, T., Stephan I, Geis-Gerstorfer, J., Sandhage, K.H., Fedorov, A.G., Rupp, F., Boyan, B.D., Tannenbaum, R., Schwartz, Z., "The roles of titanium surface micro/nanotopography and wettability on the differential response of human osteoblast lineage cells," Acta Biomater., 9(4), pp. 6268-77 (2013).

[15] Gittens, R.A., Olivares-Navarrete, R., McLachlan, T., Cai, Y., Hyzy, S.L., Schneider, J.M., Schwartz, Z., Sandhage, K.H, Boyan, B.D., "Differential responses of osteoblast lineage cells to nanotopographically-modified, microroughened titanium-aluminum-vanadium alloy surfaces," Biomaterials., 33(35), pp. 8986-8994 (2012).

CHAPTER 4

4.1 Introduction

Synthetic hydroxyapatite (HA) has intrinsic characteristics imparted from its molecular structure ($Ca_{10}(PO_4)_6(OH)_2$) similar to that of bone mineral [1] and is often explored as a bone graft substitute or as an implant material for hard tissue applications. Bone mineral differs in many ways from synthetic HA, however, particularly with respect to the presence of metal ions, including silicate [1]. The exact biological role of silicate in bone health is unclear.

The mechanisms by which silicate regulates mineralization are not well understood. It has been implicated in the synthesis of collagen and its stabilization, as well as its involvement in matrix mineralization [1,2]. It has been identified at trace levels in immature bone, suggesting that it plays a metabolic role in new bone formation [1,2]. *In vitro* and *in vivo* studies by Carlisle et al. have shown that silicate was localized in active growth areas, such as the osteoid of young bone in rats and mice, where silicate levels of up to 0.5 wt% were observed [2]. Elevated levels of silicate (up to 1.0 wt%) have been identified in mineralizing osteoid and silicate deficiencies have been associated with compromised mineralization of long bones, supporting this hypothesis [1,2,3]. Silicate substitution also has been shown to alter the surface charge and microstructure of calcium phosphate [2,3,4]. Studies by Gibson et al. have shown that non-porous silicate -substituted calcium phosphate enhances biologic response in vivo as compared to hydroxyapatite alone [3,4,5].

Several studies have shown that silicate may increase the rate of bone mineralization and enhance calcium deposition in bone, allowing bone to develop faster

and with greater integrity and mechanical strength [3,4,5]. In bioactive glass, the formation of Si-OH bonds, the condensation and repolymerization of the SiO_2-rich layer on the surface of the glass, and the formation of a calcium phosphate layer on top of the SiO_2-rich layer are all believed to initiate key mineralization and biological processes [3,4,5,6]. For this reason, it has been incorporated into bone implant materials where osteointegration is a desired outcome [5,6].

Silicated hydroxyapatites with varying silicat content have also been developed as bone graft materials. Studies by Hing et al. suggest that the microstructure and chemistry of these materials may support de novo bone formation due to apatite nucleation on the surface [7,8,9,10]. Their silicate content also affects the rate, quality and progression of bone healing in clinical applications [11], suggesting a direct effect on osteoblast biology.

In the current study, tetraethyl orthosilicate $Si(OC_2H_5)_4$, a soluble form of silica, was used to incorporate silicate into the HA lattice, without replacement of either the phosphate or hydroxyl group. Si-HA powders were created, and Si-HA discs were pressed and used as the experimental model in order to evaluate the effect silicon incorporated HA has on osteoblast-like cellular behavior.

4.2 Materials and Methods

4.2.1 HA Disc Design and Preparation

Pure hydroxyapatite with a Ca/P molar ratio of 1.78 and silicate substituted HA discs are the surface components of the experimental model. The pure hydroxyapatite powder was prepared by an aqueous precipitation reaction between a calcium nitrate solution and a diammonium hydrogen phosphate ($(NH_4)_2HPO_4$) solution. The silicate

incorporated hydroxyapatite powders were prepared by aqueous precipitation reaction between a calcium nitrate solution, an $(NH_4)_2HPO_4$ solution, and three different concentrations of $Si(OC_2H_5)_4$. The silicate was added to the phosphate group without replacement. $Si(OC_2H_5)_4$ is a soluble source of silica, which yields a fine particle size of silicate. Varying concentrations of silicate were created ranging from 2.50, 6.97, and 8.37 weight percents, designated as S1, S2, and S3 respectively.

The reaction temperature was maintained at 60°C and the pH was maintained at 11. The settled precipitate was aged for 1 hour at 60°C. After aging, the white precipitate was left overnight and then decanted, centrifuged, and washed with NH_4NO_3 and distilled water until the ammonia and all residual free calcium salts were removed. Each of the above prepared precipitates was dried at 80°C and then milled to a particle size between 1 and 8μm.

The pure and silicate incorporated hydroxyapatite powders were pressed into 17mm discs prior to firing. During the firing process, the discs shrank approximately 18%, which was accounted for in order to produce approximately 14 mm discs for cell culture. One gram of powder for each ionic concentration was used to press an individual disc and 500 μls of polyvinyl alcohol (PVA) was used as a binder to coalesce the powder. These discs were preheated to 200°C prior to firing to prevent charring and cracking. After pre-heating, the discs were then sintered to improve their compactness and integrity, ensuring they remain intact during cell culture. The discs were fired using a controlled temperature schedule that heated them from room temperature to 500°C at an initial 5°C/min rate up to 200°C, and then at a 1°C/min rate until the final temperature

was reached. Once fired, the discs were cooled similarly at a 1°C/min rate in order to prevent potential charring and cracking, and to ensure the removal of the PVA binder.

4.2.2 Sterilization of Discs

The discs were soaked and washed twice for 3 hours in 50mM ammonium bicarbonate prior to sterilization. After drying the discs in a conventional oven heated to 100°C, both sides of the discs were sterilized using an oxygen plasma cleaner (PDC-32G Harrick Oxygen Plasma, Ithaca, NY). Discs were then placed in sterile non-tissue culture treated polystyrene plates for use in the following cell culture studies described below. The cells were then soaked in the culture media containing Dulbecco's modified Eagle medium (DMEM) containing 10% fetal bovine serum (FBS) and 1% penicillin/streptomycin for 24 hours prior to cell culture to prepare the surfaces for cell seeding.

4.2.3 Characterization of Silicate Incorporated Hydroxyapatite Discs

All hydroxyapatite powder and discs were imaged by scanning electron microscopy (SEM) using the LEO 1530 SEM (LEO Electron Microscope, Oberkochen, Germany). Discs were sputter-coated with palladium-gold prior to scanning. All images were collected at a 4000x magnification using an 8kV laser. Energy dispersive X-ray spectroscopy (EDS) was used on uncoated powder and pressed samples to determine surface chemical composition of each silicated apatite.

XRD was conducted on both powder and pressed samples while being heated in order to determine the approximate temperature at which phase transition of hydroxyapatite powder may occur. For S1, S2, and S3 discs, decomposition of

hydroxyapatite into $CaCO_3$ began to occur around 700 to 750°C. The potential phase transitions and crystallinity of S1, S2, and S3 were analyzed using Cu $K_{\alpha 1}$ radiation (λ=1.54056 A) at a scanning rate of 2 $min^{-1.}$

The surface roughness of the fired hydroxyapatite discs was determined using a mechanical stylus profiler KLA-Tencor Profilometer. R_A values were determined by scanning three different sections of the surfaces for the S1, S2, and S3 experimental discs however the sides of the surfaces were not assessed. The wettability of each surface was evaluated by determining the angle at which water contacted its surface. A droplet of water, approximately 500 μls, was dispensed on the surface of each type of mineralized disc. Two different discs for each state of mineralization were evaluated. The hydrophobic or hydrophilic nature of each surface was characterized using KSV Instrument CAM 101 software.

4.2.4 Cell Culture

Human osteoblast-like MG63 cells (American Type Culture Collection, Rockville, MD) were grown on tissue culture treated polystyrene (TCPS) and on pure and silicated HA in non-tissue culture treated 24-well plates. The cells were cultured in Dulbecco's modified Eagle medium (DMEM) containing 10% fetal bovine serum (FBS) and 1% penicillin/streptomycin at 37°C in an atmosphere of 5% CO_2 and 100% humidity. Non-tissue culture treated plates were used in order to discourage cell attachment to the walls of the wells, allowing all growth factors evaluated in the media to be produced exclusively from cells attached to the surface of the discs. MG63 cells were added to the 24 well plates at a cell seeding density of 20,000/cm^2 in 500μls of media per well. Wells

containing the control MG63 cells plated on the TCPS were used as a measure of the cells reaching confluence. Media were changed at 72 hr intervals until cells reached confluence on TCPS, at which time the cells on all discs were treated as described below.

4.2.5 Cell Response

Cell number was determined in all cultures 24 hours after cells on tissue TCPS reached confluence. Cells were released from the surfaces by two sequential incubations in 0.25% trypsin for 10 mins at 37°C, in order to assure that any remaining cells were removed from the HA surfaces. Released cells were counted using an automatic cell counter (Z1 cell and particle counter, Beckman Coulter, Fullerton, CA).

Alkaline phosphatase-specific activity (orthophosphoric monoester phosphohydro-lase, alkaline; E.C. 3.1.) was measured in cell lysates as described previously [12]. Alkaline phosphatase is an early marker of differentiation and reaches its highest level as mineralization is initiated. Enzyme activity was assayed by measuring the release of *p*-nitrophenol from *p*-nitrophenylphosphate at pH 10.2 and results were normalized to protein content of the cell lysates. The levels of osteocalcin in the conditioned media were measured using a commercially available radioimmunoassay kit (Human Osteocalcin RIA Kit, Biomedical Technologies, Stoughton, MA) and normalized to cell number. The conditioned media were also assayed for growth factors and cytokines. Osteoprotegerin (OPG) was measured using an enzyme-linked immunosorbent (ELISA) kit (DY805 Osteoprotegerin DuoSet, R&D System, Minneapolis, MN). Vascular endothelial growth factor (VEDF-A) levels were also measured using an enzyme-linked immunosorbent (ELISA) kit (DY233 VEGF DuoSet, R&D System, Minneapolis, MN).

4.2.6 Statistical Analysis

The data presented here are from one of two separate sets of experiments. Both sets of experiments yield comparable observations. For any given experiment, each data point represents the mean±standard error of six individual cultures. Data were initially analyzed by analysis of variance; when statistical differences were detected, Bonferroni's modification student's t-test for multiple comparisons using was used. For the surface characterizations and cell response results, * represents [Sn vs. HA], + represents [S3 vs. S2], and $ represents [S3 vs. S1] where 0% silicate represents the pure HA control. p-Values<0.05 were considered to be significant.

4.3 Results

Scanning electron microscopy detected slight variations in the surface features of the HA and Si-HA surfaces (Figure 11). The HA and S1 surfaces presented relatively similar surface characteristics, while S2 and S3 appeared distinctly different from all other surfaces (Figure 11). The S2 surfaces had clusters of HA forming throughout while the S3 surface appeared to be even less homogenous with ripples of HA throughout.

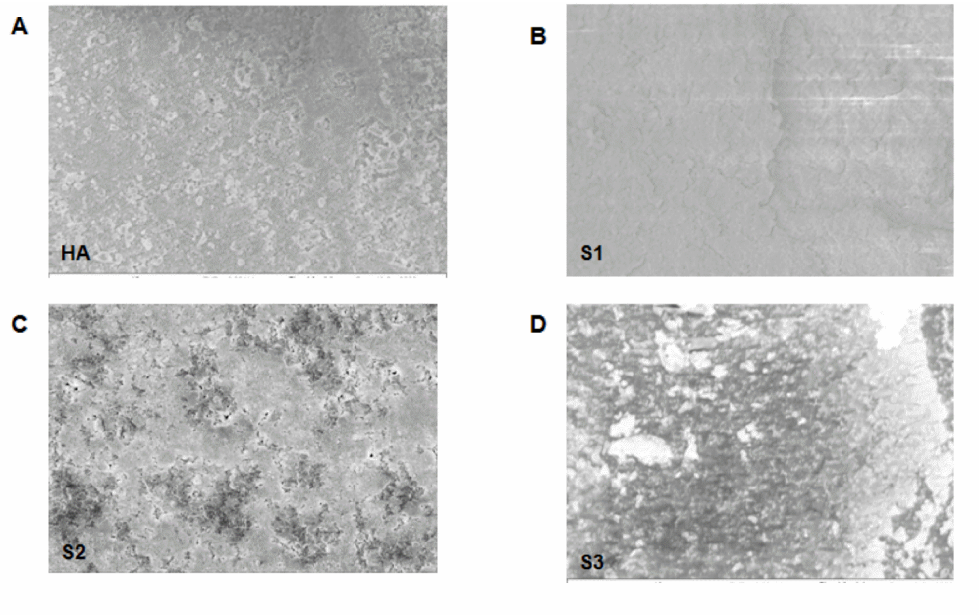

Figure 11. SEM of HA and Si-HA powders. (A) HA, (B) C1 (2.5%), (C) C2 (6.97%), (D) C3 (3.87%) were coated with gold and their surfaces were imaged at 4k X using an 8 kV power source.

Surface chemical composition vaired as a function of silicate content . Si was not present on the surfaces of pure HA discs, and increased monotonically on the Si-HA discs as the concentration of silicate in the HA lattice increased. The Ca/P ratio of the pure synthetic hydroxyapatite was approximately 1.78, within the typical range of synthetic HA (1.5 – 2.0), as was S2 and S3, with S1 being only slightly outside of the typical HA Ca/P range [8].

XRD demonstrated that the HA lattice was not disrupted upon silicate insertion (Figure 12). The crystal X-ray diffraction patterns for S1, S2 and S3 mirror that of standard stoichiometric synthetic HA.

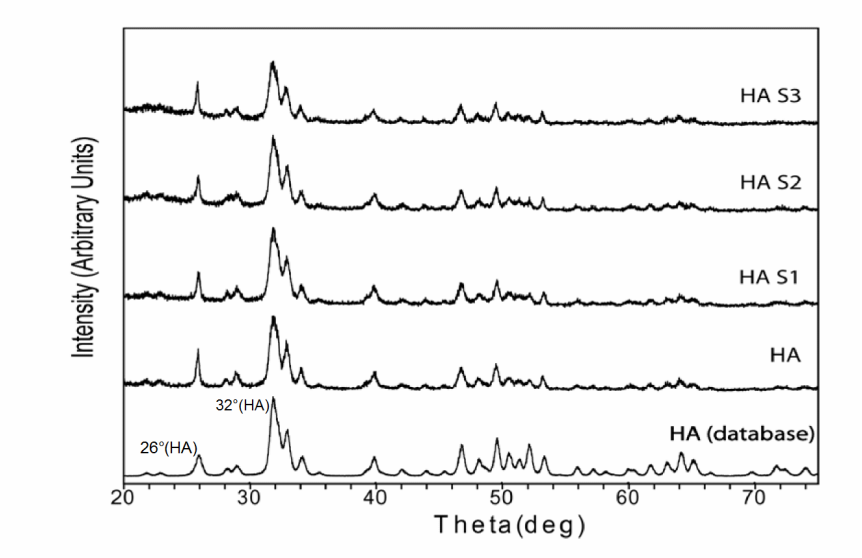

Figure 12. XRD analysis of HA and Si-HA discs. The phase of the fired Si-HA discs was analyzed using Cu $K_{\alpha 1}$ radiation (λ=1.54056 A) at a scanning rate of 2 min $^{-1}$. The phase of the fired Si-HA is compared to the standard phase of hydroxyapatite.

Surface roughness was greatest on the pure HA surfaces. Incorporation of Si reduced R_A, however, it increased with increasing silicate content (Figure 13a). Additionally, all Si-HA substitutes were found to be relatively hydrophilic, having a contact angle less than 90°C. However, S1 had the largest contact angle and thereby least wettability—approaching hydrophobicity. We observed that the wettability of all Si-HA substitutes significantly increased with increasing silicate content (Figure 13b).

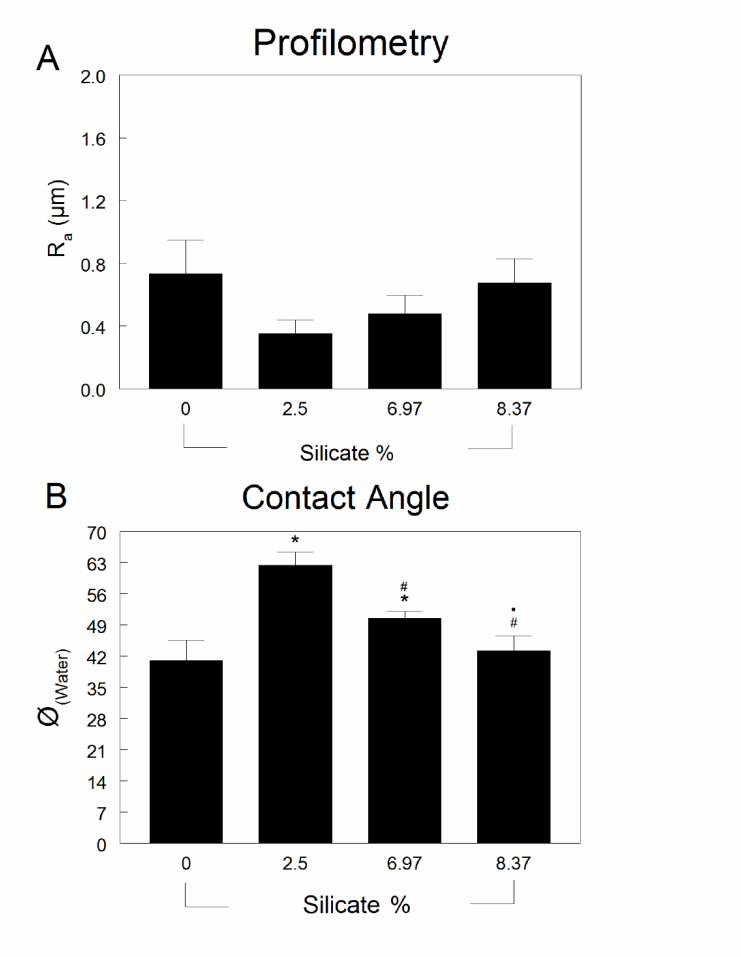

Figure 13. Surface roughness and wettability of HA and Si-HA discs. (A) R_A values were determined for pure HA and Si-HA substitutes. (B) Contact angles of pure HA and Si-HA substitutes. Values are mean±SEM of an experiment with n=6. Data were analyzed by ANOVA and significant differences between groups determined using the Bonferroni modification of Student's *t*-test.

Cell number was sensitive to Si content of the discs (Figure 14a). HA discs supported the smallest number of cells whereas discs with Si content had the greatest number of cells. Higher Si concentrations correlated with increasing cell number compared to HA but levels were still significantly lower than 2.5% Si (Figure 14a). Cell number was inversely correlated with alkaline phosphatase activity (Figure 14b) and osteocalcin production (Figure 14c).

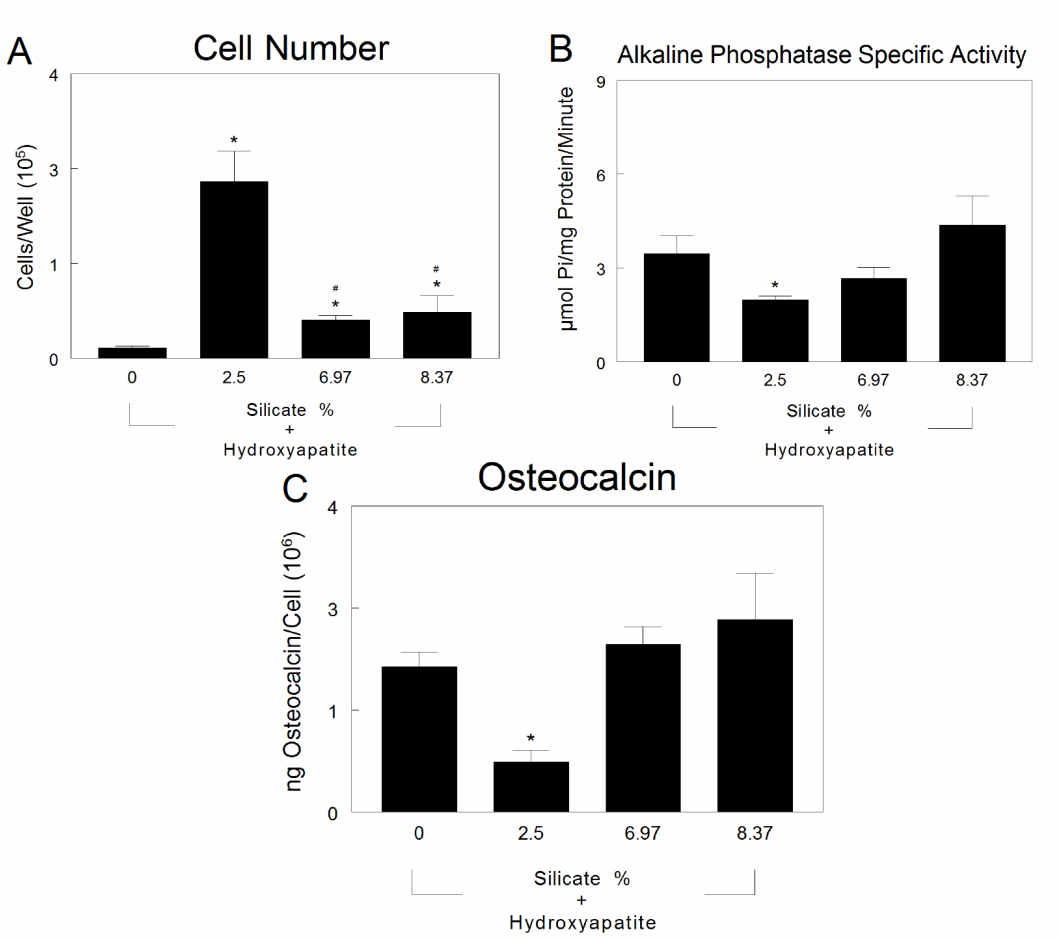

Figure 14. Interactions of MG63 cells cultured on HA and Si-HA discs. (A) Cell number was measured 24 hrs after cells reached confluence on surfaces. (B) Alkaline phosphatase-specific activity was measured in harvested cells and (C) osteocalcin levels were measured in conditioned media of confluent cultures. Values are mean±SEM of six independent cultures. Data are from one of three separate experiments, with comparable results. Data were analyzed by ANOVA and significant differences between groups determined using the Bonferroni modification of Student's *t*-test.

OPG levels on pure HA discs were comparable to those for the S2 and S3 surfaces (Figure 15a). In contrast, cells on the S1 surface produced significantly lower levels of the protein. VEGF-A production, however, was insensitive to surface chemistry (Figure 15b).

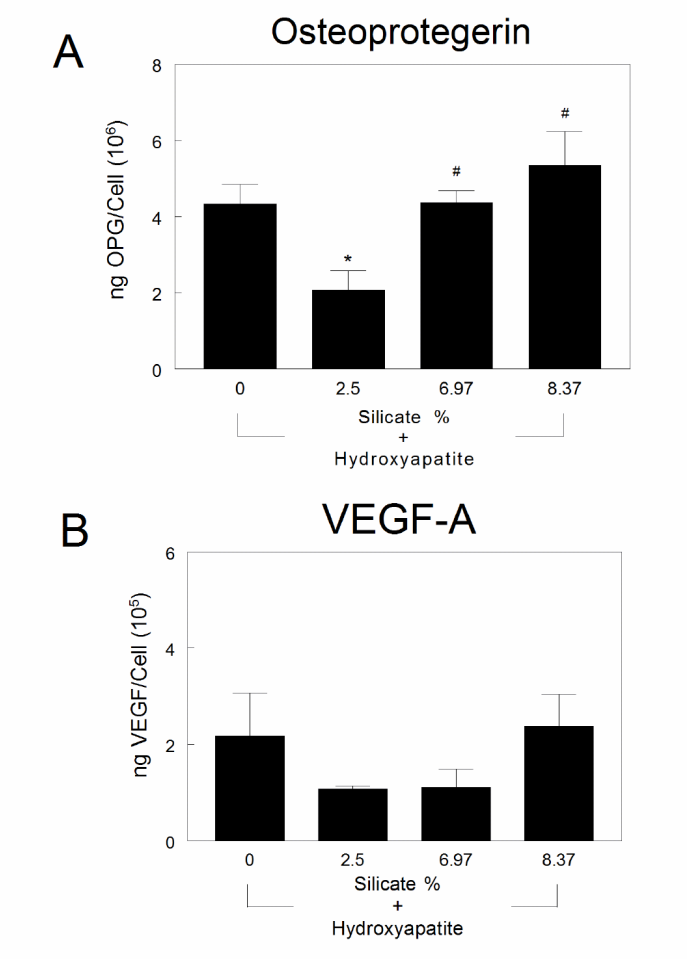

Figure 15. Effect of HA and Si-HA discs on MG63 cell production of OPG and VEGF-A. (A) Osteoprotegerin in the conditioned media was assayed and measured. (B) Vascular Endothelial GF levels were also measured in conditioned media of confluent cultures. Data are from one of three separate experiments, with comparable results. Data were analyzed by ANOVA and significant differences between groups determined using the Bonferroni modification of Student's *t*-test.

4.4 Discussion

This study demonstrated that silicate was incorporated into hydroxyapatite (Si-HA) without altering the Ca/P ratio of pure HA. Moreover, the increase in silicate concentration corresponded to an increase in percent weight of silicate for each substitute. The incorporation of silicate ions into hydroxyapatite, as opposed to substitution of silicate replacing either the phosphate or hydroxyl groups, caused no disruption in the crystallinity of the hydroxyapatite lattice. Characteristic hydroxyapatite peaks at 26˚ and 32˚, respectively, were maintained and clearly observed by X-ray diffraction analysis, presenting no detectable transition in phase.

The surfaces of the Si-HA discs were not significantly rough and displayed only slight differences amongst the discs with varying silicate concentrations. Thus, changes in cell response were not attributable to surface texture [3]. Surface chemistry was affected by incorporation of silicate, however. The S1 surface was more hydrophic than HA, S2 or S3, although all four substrates were hydrophilic in nature. A number of studies suggest that wettability is an important variable in determining osteoblast response to a material surface, and indicate that hydrophobic surfaces are more osteogenic [3,13].

Interestingly, the lowest Si-HA surface, S1 supported greater cell numbers but reduced differentiation compared to pure HA. Moreover, neither S2 nor S3 enhanced osteoblast differentiation compared to HA. This is in contrast to reports that silicated HA supports enhanced bone healing [7,8,9,10] or that bioglasses stimulate osteoblast differentiation [3,4,5]. The apparent discrepancy suggests that Si content alone is not critical, but how it is presented to the cells is important. Osteoprotegerin was also

sensitive to Si content but no difference in VEFG-A production was observed, indicating that factor production is differentially regulated by cell/material interactions.

While the exact biological role of silicate in bone formation is still unclear, silicate has been identified at trace levels in immature bone and is believed to play a metabolic role in new bone formation. In the current study, tetraethyl orthosilicate was used to incorporate silicate into the hydroxyapatite (HA) powder to produce silicate incorporated HA (Si-HA) powder; Si-HA powders at varying concentrations were pressed into discs and used as the experimental model in order to evaluate the effect silicate incorporated HA has on osteoblast-like cell behavior. The incorporation of silicate ions into the hydroxyapatite powder, as opposed to the substitution of silicate replacing either the phosphate or hydroxyl groups, caused no disruption in the crystallinity of the hydroxyapatite lattice. There was no significant difference in surface microscale roughness amongst the Si-HA discs with varying silicate concentrations. Cell number varied with Si content, with the greatest number of cells on discs with the lowest Si content. In contrast, osteoblastic differentiation (alkaline phosphatase, osteocalcin) was greatest on substrates with the highest Si content, but was not greater than pure HA. Osteoprotegerin levels also varied in response to the increase in silicate content, whereas vascular endothelial growth factor-A was not affected by the presence of silicate in the HA lattice. These results suggest that osteogenic properties of HA-based bone graft materials may be modified by incorporating silicate into the HA-lattice.

4.5 References

[1] Patel N, Best S, Bonfield W. A comparative study on the in vivo behavior of hydroxyapatite and silicon substituted hydroxyapatite granules. J Mater Sci Mater Med. 13(12), pp.1199-1206 (2002).

[2] Carlisle, E.M., "Silicon: A possible factor in bone calcification," Science, vol.167, pp. 179-280 (1970).

[3] Gibson, I.R., Best, S.M., Bonfield W., "Chemical characterization of siliconsubstituted hydroxyapatite," J Biomed Mater Res., 44(4), pp. 422-428 (1998).

[4] Begley, C.T., Doherty M.J., Hankey, D.P., Wilson, D.J., "The culture of human osteoblasts upon bone graft substitutes," Bone, vol.14, pp. 661-666 (1993).

[5] Yuan, H., et al., "Osteoinduction by calcium phosphate biomaterials," J Mater Sci Mater Med., 9(12), pp. 723-726 (1998).

[6] Webster, T.J., Ergun, C., Doremus, R.H., Siegel, R.W., Bizios, R., "Enhanced functions of osteoblasts on nanophase ceramics," Biomaterials, vol. 21, pp. 1803-1810 (2000).

[7] Campion, C.R., Ball, S.L., Clarke, D.L., Hing, K.A., "Microstructure and chemistry affects apatite nucleation on calcium phosphate bone graft substitutes," J Mater Sci Mater Med., 24(3), pp. 597-610 (2013).

[8] Chan, O., Coathup, M.J., Nesbitt, A., Ho, C.Y., Hing, K.A., Buckland, T., Campion, C., Blunn, G.W., "The effects of microporosity on osteoinduction of calcium phosphate bone graft substitute biomaterials," Acta Biomater., 8(7), pp. 2788-94 (2012).

[9] Coathup, M.J., Hing, K.A., Samizadeh, S., Chan, O., Fang, Y.S., Campion, C., Buckland, T., Blunn, G.W., "Effect of increased strut porosity of calcium phosphate bone graft substitute biomaterials on osteoinduction,". J Biomed Mater Res A., 100(6), pp. 1550-1555 (2012).

[10] Coathup, M.J., Samizadehm S., Fang, Y.S., Buckland, T., Hing, K.A., Blunn, G.W., "The osteoinductivity of silicate-substituted calcium phosphate," J Bone Joint Surg Am., 93(23), pp. 2219-26 92011).

[11] Guth, K., Campion, C., Buckland, T., Hing, K.A., "Effects of serum protein on ionic exchange between culture medium and microporous hydroxyapatite and silicate-substituted hydroxyapatite," J Mater Sci Mater Med., 229(10), pp. 2155-2164 (2011).

[12] Bretaudiere, J.P., Spillman T., Methods of Enzymatic Analysis., Bergmeyer, Germany: Verlag Chemica., vol. 4, pp75-92, (1984).

[13] Weiner, S., Wagner, H.D., “The material bone: structure mechanical function relations,” Annual Review of Materials Science, vol. 28, pp. 271-298 (1998).

CHAPTER 5

5.1 Introduction

Physiological bone matrix is a composite material consisting primarily of type I collagen and the nano-biomineral, carbonated hydroxyapatite. While the exact mechanism by which mineral is deposited within the collagen fibrils is not known, recent studies on developing fin bone in zebrafish have shown that it involves an amorphous precursor [1-2]. Once the amorphous phase interpenetrates throughout the interstices of the fibril, it crystallizes, leaving nanocrystals of hydroxyapatite extending throughout the fibril network [3]. The resulting nanostructured composite has both compressive and tensile load-bearing properties [4]. In addition, the poorly crystalline nature of the mineral makes it more labile than crystalline hydroxyapatite, which is important for its role as a physiologically responsive source of calcium and phosphate [5].

Synthetic bone graft substitutes have used various calcium phosphate compositions to mimic bone mineral, resulting in different three-dimensional morphologies and different degradation rates [6-7]. However, they lack the biological properties of the nanostructured composite present in bone. In order to overcome these limitations, Gower and colleagues [3,8] developed a bovine type I collagen and synthetic calcium phosphate nanostructured composite using a polymer-induced liquid-precursor (PILP) process. They found that adding micro-molar quantities of anionic polypeptides (such as polyaspartic acid- sodium salt) to the supersaturated crystallizing solution created nano-droplets of a hydrated liquid-phase mineral precursor. This charged polymer sequesters ions (or a liquid condensed phase of ions), thereby preventing crystal nucleation and inducing liquid-liquid phase separation in the crystallizing solution [9]. It

has been hypothesized that the fluidic amorphous phase is drawn into the network of collagen fibrils through capillary action, leading to intrafibrillar mineralization [3]. A thin coating of extrafibrillar mineral may also form on the surface of the fibrils, leading to a combination of intra- and extra-fibrillar mineral, as is found in bone. The precursor phase then crystallizes; leaving calcium phosphate nanocrystals embedded within the collagen fibrils, thereby creating composites that mimic the nanostructure of secondary bone [3]. Cryo-transmission electron microscopy (cryoTEM) studies using this model system (with polyaspartate additive) have shown that the droplets (or amorphous particles) adsorb to specific bands on the collagen, and the collagen may further initiate the crystallization of the amorphous phase once it is within the fibril [3].

Studies using fully dense and sintered calcium phosphate substrates to examine osteoblast differentiation *in vitro* have shown that osteoblast differentiation is enhanced compared to osteoblasts grown on tissue culture polystyrene (TCPS) [11]. While the intent of these calcium phosphate substrates is to provide a more physiological environment for the osteoblasts than TCPS, the mineral phase that is presented to the cells has little in common with the formatting of mineral on the bone surface colonized by osteoblasts *in vivo*.

Other studies have shown that the crystallinity and size of the calcium phosphate can also be important variables in determining cell response [12-14]. The purpose of the study herein was to determine if osteoblasts are sensitive to the manner in which mineralized collagen is formatted. To do this, human osteoblast-like MG63 cells were cultured on type I collagen/hydroxyapatite composites prepared using the PILP technology, where the collagen fibrils have nanocrystals intercalated within the fibrillar

structure, and compared to composites mineralized using a conventional calcium phosphate solution (lacking the anionic polypeptides that induce the PILP process), where collagen is simply coated with spherulitic clusters of mineral on the surface. To further examine the mechanisms mediating the effects of the collagen/mineral composites on osteoblast differentiation, MG63 cells that were stably silenced for the alpha α2-integrin subunit were used, since α2β1-integrins target collagen and signaling via this integrin pair which induces osteoblast differentiation [15].

5.2 Materials and Methods

5.2.1 Type I Collagen and Calcium Phosphate Composites

5.2.1.1 Preparation

Collagen/nanostructured calcium phosphate composite sponges were produced using the polymer-induced liquid-precursor (PILP) process. The mineralizing solution was prepared by mixing equal volumes of 9 mM $CaCl_2$ solution in Tris buffer (pH 7.4) and 4.2 mM K_2HPO_4 solution in Tris buffer (pH 7.4), to final concentrations of 4.5 mM Ca and 2.1 mM phosphate. Polyaspartic acid•sodium salt (Sigma: M.W. of 10,500 Da) was added to the mineralizing solution to achieve a 50 μg/ml concentration of the process-directing agent. Each solution was adjusted to a pH of 7.4 using 0.1 N NaOH or HCl. Collagen sponges were obtained from two different sources: Batch A, Collagen Matrix, Inc. (www.collagenmatrix.com) and Batch B, ACE Surgical Supply, Inc. (www.acesurgical.com) due to a limited supply of Batch A. The sponges were placed in the crystallizing solution, placed under vacuum for 30 minutes to remove air bubbles, and then incubated at 37^{o}C for 14 days to simulate physiological conditions. After mineralization, the sponges were removed and rinsed with distilled water three times

(with gentle stirring for 30 minutes) and ethanol to remove extraneous salts. The samples CSPILP were then dried in air at room temperature [3].

Type I collagen sponges were also incubated in the calcium phosphate solution without addition of polyaspartate, for the preparation of the control CSHA samples.

5.2.1.2 Characterization

Dried samples of Batch A sponges were sputter coated with palladium-gold and imaged by scanning electron microscopy (LEO 1530 Scanning Electron Microscope [SEM], Oberkochen, Germany). Batch A sponges were also analyzed using transmission electron microscopy (TEM) and selected area electron diffraction (SAED). The samples were crushed into a fine-grained powder in a liquid nitrogen mortar and pestle. A few drops of ethanol were added to the powder, and this slurry was transferred to a 3mm diameter carbon/Formvar coated copper TEM grid. The samples were then sputter coated with a thin layer of amorphous carbon and then analyzed using 200CX JEOL TEM at 200kV in brightfield, darkfield and SAED modes as described previously [3,15].

The degree of mineralization of the non-PILP HA collagen sponge (CSHA) and the PILP HA collagen sponge (CSPILP) was determined by employing thermogravimeteric analysis (TGA). The mineral ash content was determined by heating the CSHA and CSPILP sponges up to 800°C, thereby eliminating all organic material. The crystallinity of the collagen sponge surfaces was determined by X-ray diffraction

(XRD) using a Philips XRD ADP 3720 Diffractometer with Cu-Kα radiation at 40 KV and 20 mA, using a step size of 0.011θ mrad/s with a time of 1.25 s/step.

5.2.2 Cell Culture Model

MG63 human osteoblast-like cells were purchased from the American Type Culture Collection (Rockville, MD). Cells were grown to confluence and then sub-cultured onto the Batch A test surfaces in a 24-well tissue culture plate. Non-tissue culture treated plates were used to discourage cell attachment to the walls of the wells, allowing all growth factors evaluated in media to be exclusively from cells attached to the wafer or composite. Cells were seeded in the tissue culture plate at 20,000/cm^2 in 500μls of Dulbecco's modified Eagle medium (DMEM) containing 10% fetal bovine serum (FBS) and 1% penicillin/streptomycin and were grown at 37°C in an atmosphere of 5% CO_2 and 100% humidity. Media were changed at 72 hour intervals until cells reached confluence, at which time the cells were harvested.

Sterile CellCrown 24-well inserts (Scaffdex, Inc.) were used to immobilize the collagen scaffolds and for this reason the control cultures grown on non-tissue culture polystyrene (TCPS) also containing the inserts, to eliminate any contribution the inserts might have on the cultures. Prior to insertion the medical grade polycarbonate inserts were autoclaved. All inserts and collagen sponges were exposed to ultraviolet light overnight prior to adding the cells. Only uniformly sized collagen sponges were used. In addition, by including the inserts in the control cultures, all cells were exposed to constructs of comparable size. The collagen scaffolds were also exposed to ultraviolet radiation 24 hours prior to cell seeding.

To assess the role of α2β1-signaling, we used an MG63 cell line that was stably silenced for α_2. This cell line was generated by transfection with α2 integrin shRNA using a P-suppressor-neo vector system and shown to have a 70% reduction in α2 protein [16]. The α2-silenced MG63 cells were maintained in medium containing Geneticin® (G418; Invitrogen, Carlsbad, CA) at a concentration of 600 μg/mL. Experiments using these cells were conducted on Batch B scaffolds.

5.2.3 Cell Response

Cell number was determined in all cultures 24 hours after cells on TCPS reached confluence. Because of the opacity of the collagen sponges, we were not able to determine if cells were also at confluence on them and therefore, it was possible that the cells were at different states of confluence at the time of harvest than those cells on TCPS. However, we have found that by standardizing all cultures against the 24 hour post confluence on TCPS time point, we can observe reproducible results between repeated experiments [16]. Cells were released from the surfaces by two sequential incubations in 0.25% trypsin for 10 minutes at 37°C, in order to ensure that any remaining cells were removed from the mineralized sponges. Although some cells may have traveled into and throughout the porous substrates, the monolayer of cells on the substrate surfaces was released and counted using an automatic cell counter (Z1 cell and particle counter, Beckman Coulter, Fullerton, CA) for comparison to the monolayer of cells extracted from the control group.

We used two determinants of osteoblast differentiation: alkaline phosphatase specific activity (orthophosphoric monoester phosphohydrolase, alkaline; E.C. 3.1.3.1) of

cell lysates, and osteocalcin content of the conditioned media. Alkaline phosphatase is an early marker of differentiation and reaches its highest level as mineralization is initiated. Osteocalcin is a late marker of differentiation and increases as mineral is deposited.

Cells were lysed by sonicating them in phosphate buffered saline (PBS) three times for 10 seconds, and enzyme activity was assayed by measuring the release of *p*-nitrophenol from *p*-nitrophenylphosphate at pH 10.2. Results were normalized to protein content of the cell lysates, determined using a colorimetric assay. The levels of osteocalcin in the conditioned media were measured using a commercially available radioimmunoassay kit (Human Osteocalcin RIA Kit, Biomedical Technologies, Stoughton, MA) and normalized to cell number.

The conditioned media were also assayed for growth factors and cytokines. Osteoprotegerin (OPG) and vascular endothelial growth factor (VEGF) were measured using enzyme-linked immunosorbent (ELISA) kits (DY805 Osteoprotegerin DuoSet and DY233 VEGF DuoSet, R&D Systems, Minneapolis, MN).

5.2.4 Statistical Analysis

For any given experiment, each data point represents the mean ± standard error of the mean (SEM) for six individual cultures. Data were first analyzed by analysis of variance; when statistical differences were detected, Student's t-test for multiple comparisons using Bonferroni's modification was used. p-Values<0.05 were considered to be significant. Data from individual experiments are shown. In addition, to determine the validity of the data, the results from multiple experiments were compared using treatment/control ratios (N=3 experiments for wild type MG63 cells on Batch A scaffolds

and N=2 experiments for α2silenced cells on Batch B scaffolds).

5.3 Results

The collagen/hydroxyapatite composite sponges varied as a function of processing method, as can be seen by SEM. Control sponges (without mineral) had a continuous surface uninterrupted by crystal formation, with a few regions containing a fibrillar mesh, while most regions contained more densely packed clumps of collagen where the fibrillar texture is not easily discerned (Figure 16a). The CSHA sponges had a surface that also showed dense collagen at non-mineralized sites, speckled with regions containing spherulitic clusters of hydroxyapatite on the surface (Figure 16b). The CSPILP mineralized sponges had surfaces with a more pronounced fibrillar texture, which is commonly observed with the incorporation of intrafibrillar mineral (Figure 16c). Occasional nodules or bulges occurred along the fibrils, which is also common from non-uniform infiltration of the precursor [17]. Energy dispersive spectroscopy was used to confirm the presence of mineral (Figure 16d).

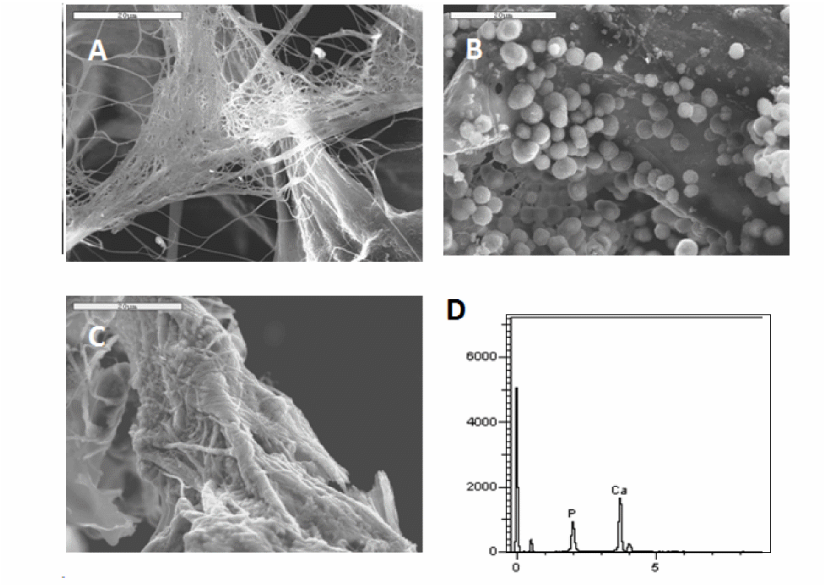

Figure 16. SEM of collagen/hydroxyapatite composite sponges. (A) collagen sponge control (CS) prior to mineralization, (B) collagen sponge mineralized without PILP (CSHA), and (C) collagen sponge mineralized using the PILP process (CSPILP). Scale bars = 20 □m. (D) XRD of collagen/hydroxyapatite composite sponges using a Philips XRD ADP 3720 Diffractometer with Cu-Kα radiation at 40 KV and 20 mA, using a step size of 0.01θ mrad/s with a time of 1.25 s/step.

Transmission electron micrographs demonstrated that the calcium phosphate crystals were aligned along the collagen fibrils (Figure 17a,b), and SAED showed that they were aligned in the [001] direction (inset of Figure 17b), as occurs in bone. The degree of mineralization of the CSHA sponge and the CSPILP sponge varied. The mineral ash content of the CSHA sponge was approximately 43% (Figure 17c), whereas the mineral content evaluated for the CSPILP sponge was approximately 66% (Figure 17d), similar to the composition of mineral within bone. XRD showed that the mineral integrated in CSPILP had the characteristic peaks of HA at 26° and 32° (Figure 17e), and the peaks were quite broad (due to small crystallite size or imperfections), which is also seen in bone.

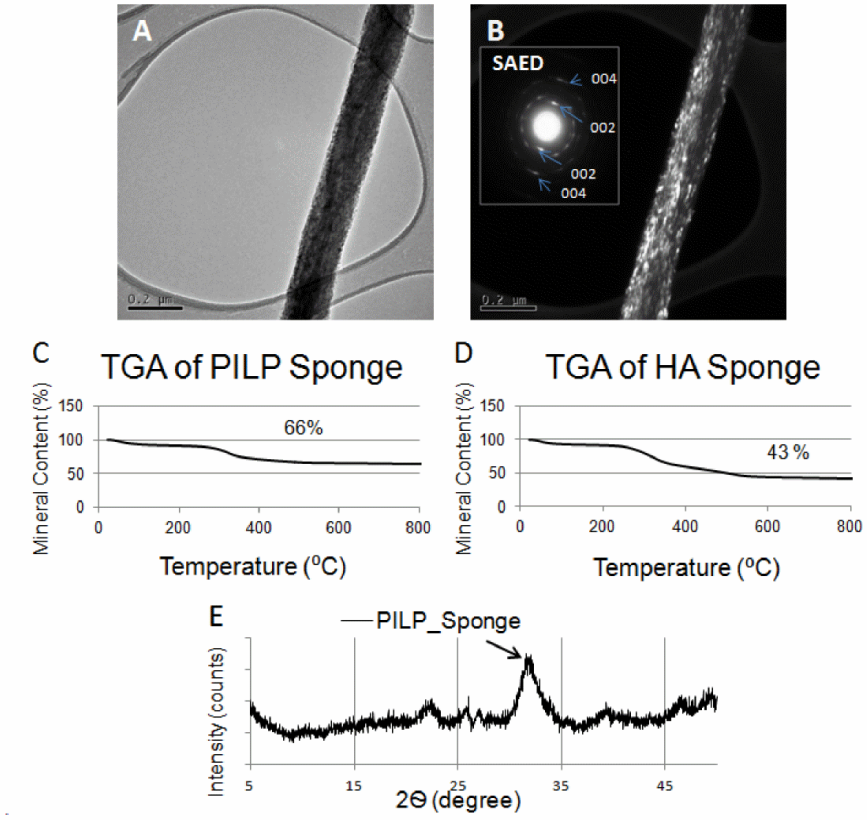

Figure 17. TEM, SAED, TGA, and XRD analysis of collagen fibrils isolated from calcium phosphate mineralized sponge using the PILP process. (A) Brightfield TEM of an isolated PILP mineralized fibril, and (B) Darkfield TEM of the same fibril highlighting the crystals that produced the (002) diffraction spots (the [001] oriented nanocrystals). The inset shows the SAED pattern used to obtain the darkfield image. The SAED pattern shows arcing of the spots, which indicates that there is some rotational and tilt disorder of the crystallites, as is also seen in bone. (C) TGA indicating degree of mineralization of CSPILP (66 wt%), and (D) TGA of CSHA composite (43 wt%). (E) XRD of the calcium phosphate mineral component in the CSPILP, which exhibits broad HA peaks, as is also seen for bone.

Cell response to Batch A sponges was sensitive to the formatting of the mineralized collagen. The number of cells observed on the CSHA surface was significantly lower than on the CSPILP surface or collagen sponge (CS) control surfaces (Figure 18a). Alkaline phosphatase specific activity of cells cultured on CS and CSPILP was greater than on CSHA, with activity observed for CSPILP being the greatest among all groups. Alkaline phosphatase measured for CSHA was comparable to that detected in the TCPS insert control group (Figure 18c). However, differentiation of the CSHA group

was greater in comparison to CSPILP and both control groups based on osteocalcin levels in the conditioned medium (Figure 18e).

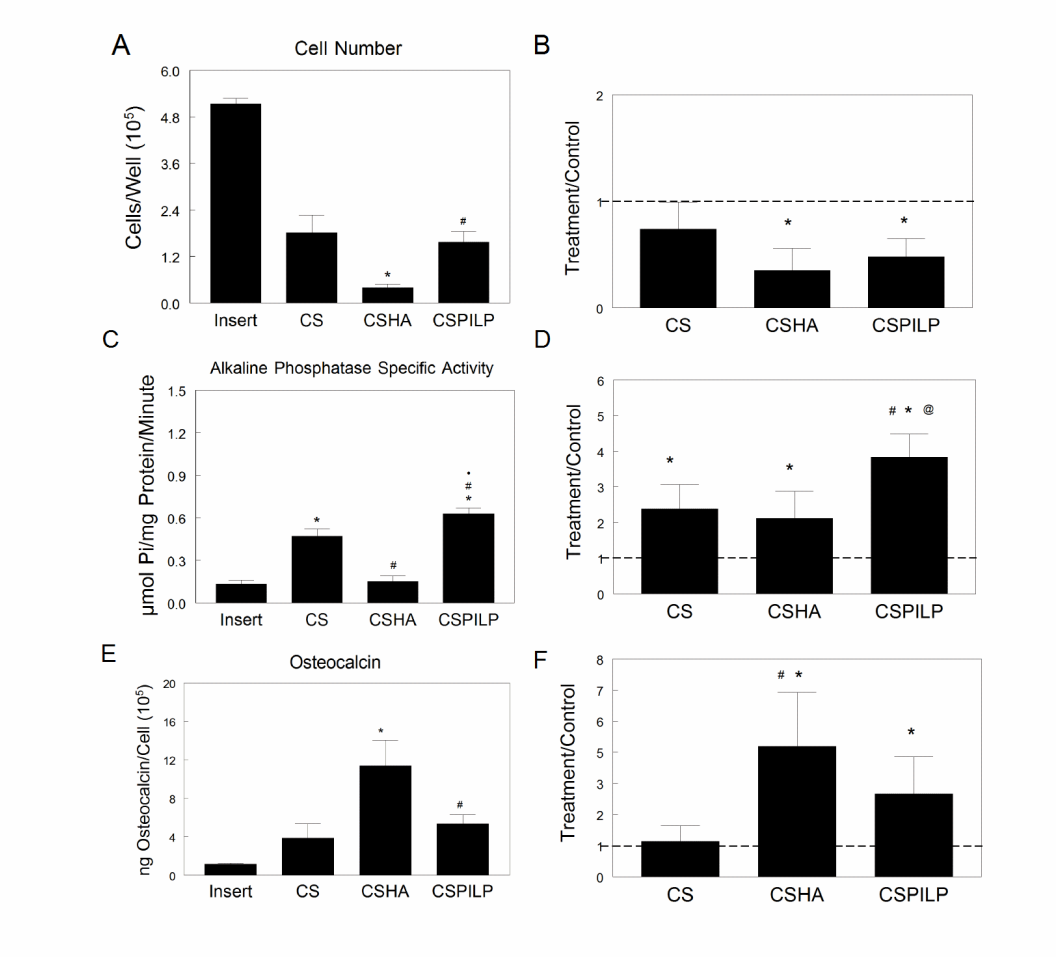

Figure 18. Interactions of MG63 cells cultured on tissue culture polystyrene (Insert), a collagen sponge control (CS), and collagen sponge mineralized without (CSHA) and with PILP (CSPILP), respectively. (A) Cell number was measured 24 hrs after cells reached confluence on the control (Insert) surfaces, where * represents [CSHA vs. CS] and # represents [CSPILP vs. CSHA]. (B) Treatment/control ratio (collagen sponge/TCPS) was determined. (C) Alkaline phosphatase-specific activity was measured in harvested cells, where * represents [CSHA vs. CS], # represents [CSPILP vs. CSHA], and · represents [CSPILP vs. CS]. (D) Treatment/control ratio was determined. (E) Osteocalcin levels were measured in conditioned media of confluent cultures, where * represents [CSHA vs. CS] and # represents [CSPILP vs. CSHA]. (F) Treatment/control ratio was determined. Values are mean ± SEM of six independent cultures. Data are from one of three separate experiments, with comparable results. Data were analyzed by ANOVA and significant differences between groups determined using the Bonferroni modification of Student's *t*-test.

Local factors were also regulated by the presentation of calcium phosphate and type I collagen. Osteoprotegerin (OPG) in the conditioned media of cells grown on CSHA was significantly greater than all other experimental groups, while OPG levels detected on CSPILP were greater than those on TCPS inserts (Figure 19a). Vascular endothelial growth factor A (VEGF-A) levels in the conditioned media of cells cultured on the CSHA surfaces were significantly less than VEGF-A levels for CSPILP or CS surfaces. VEGF-A levels for CSPILP and CS surfaces were comparable (Figure 19c).

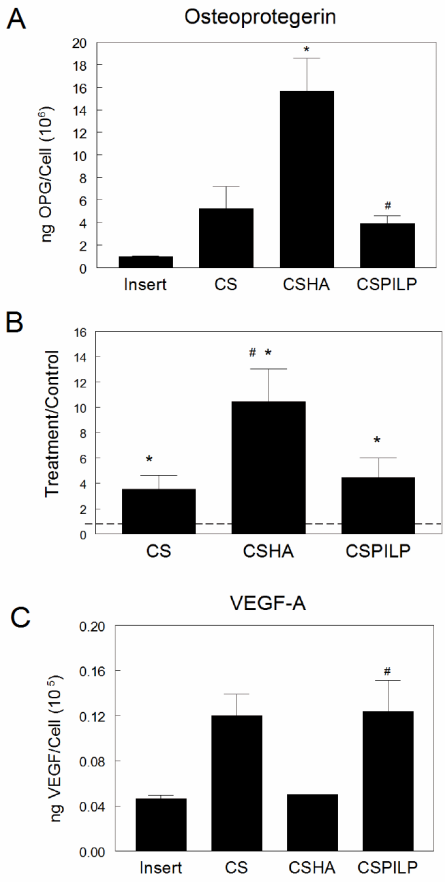

Figure 19. Effect of MG63 cells cultured on tissue culture polystyrene (Insert), a collagen sponge control (CS), and collagen sponge mineralized without (CSHA) and with PILP (CSPILP) on cell production of OPG and VEGF-A. (A) Osteoprotegerin in the conditioned media was assayed and measured, where * represents [CSHA vs. CS] and # represents [CSPILP vs. CSHA]. (B) Treatment/control ratio was determined. (C) Vascular Endothelial Growth Factor levels were measured in conditioned media of confluent cultures, where # represents [CSPILP vs. CSHA].

Response to the Batch B scaffolds was mediated by α2β1-signaling (Figure 20a). MG63 cell numbers were reduced on all collagen sponges compared to TCPS inserts, with the greatest reductions seen on the mineralized sponges. The cell numbers for α2-silenced MG63 cells were increased over wild type MG63 cells cultured on TCPS insert control, CSHA and CSPILP surfaces but were comparable on control collagen sponges (CS). Osteocalcin content of the conditioned media was comparable in cultures of wild

type and α2-silenced MG63 cells grown on TCPS or on CS sponges. Both wild type and α2-silenced cells exhibited marked increases in osteocalcin when grown on the mineralized sponges, but the effect was attenuated in the α2-silenced cells. The inhibitory effect of α2-silencing was less pronounced in cultures grown on CSPILP compared to CSHA (Figure 20b).

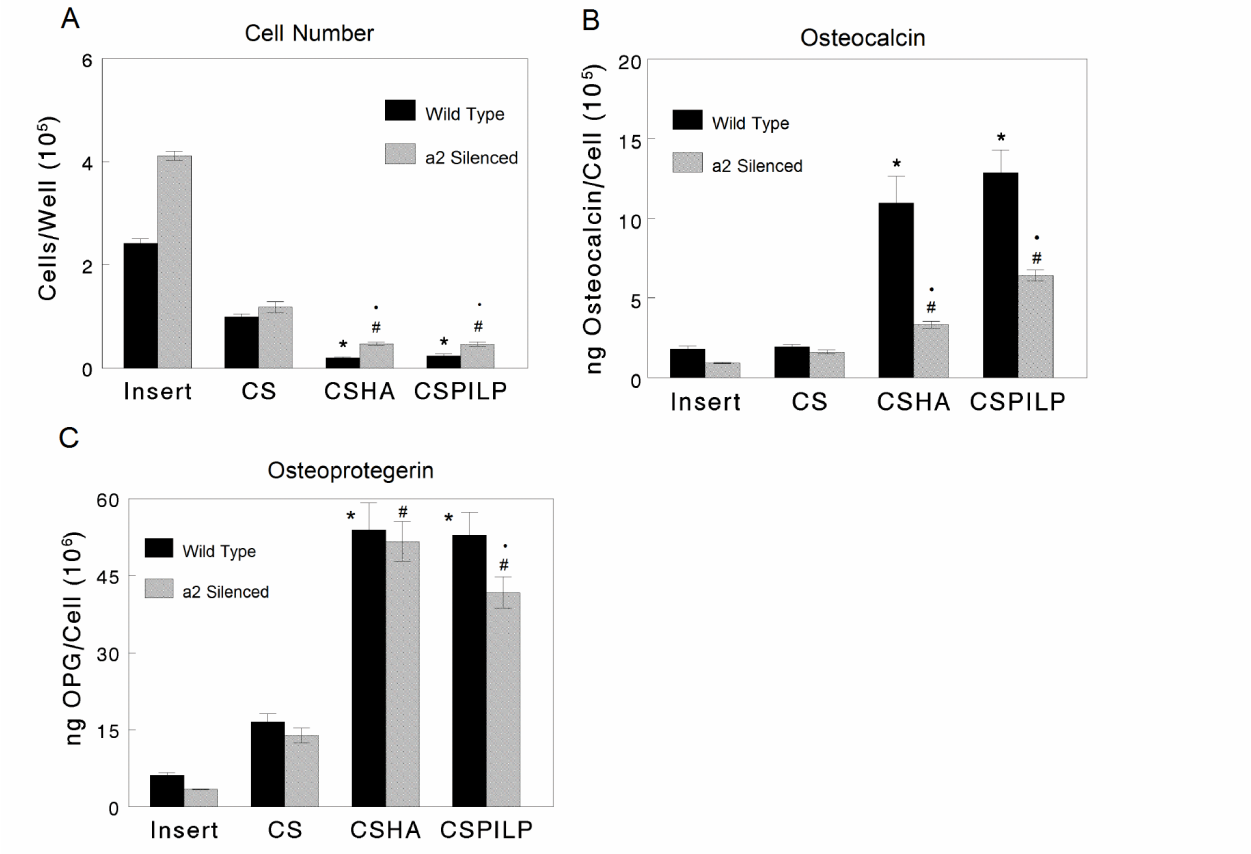

Figure 20. Comparison of the effects of CS, CSHA, and CSPILP on wild type versus α2-silenced MG63 cells. (A) Cell number was measured 24 hrs after cells reached confluence on tissue culture polystyrene (Insert) surfaces, where *represents [wtCSHA, wtCSPILP vs. wtCS], # represents [α2-silencedCSHA, α2-silencedCSPILP vs. α2-silencedCS], · represents [wt vs. α2-silenced]. (B) Osteocalcin levels were measured in conditioned media of confluent cultures, where * represents [wtCSHA, wtCSPILP vs. wtCS], # represents [α2-silencedCSHA, α2-silencedCSPILP vs. α2-silencedCS] , and · represents [wt vs. α2-silenced]. (C) Osteoprotegerin in the conditioned media was assayed and measured where, * represents [wtCSHA, wtCSPILP vs. wtCS], # represents [wtCSHA, wtCSPILP vs. wtCS] and, · represents [wt vs. α2-silenced]. Values are mean ± SEM of six independent cultures. Data are from one of three separate experiments, with comparable results. Data were analyzed by ANOVA and significant differences between groups determined using the Bonferroni modification of Student's *t*-test.

Production of osteoprotegerin was also sensitive to the substrate. OPG was increased in the conditioned media of both wild type and α2-silenced MG63 cells on all collagen sponges compared to TCPS inserts, with the greatest increases on the mineralized collagen sponges. The effect was attenuated in the media of α2-silenced cells grown on CSPILP sponges (Figure 20c).

5.4 Discussion

Hydroxyapatite integrated collagen sponges provide a physiologic presentation of the organic and inorganic components analogous to bone matrix [3,8]. Microscopic evaluation of type I collagen sponges (CS), type I collagen sponges with a hydroxyapatite surface coating (CSHA), and type I collagen sponges with intrafibrillar hydroxyapatite (CSPILP) showed that both HA and fibrillar collagen were exposed on the surfaces of all of the materials, particularly when using the PILP process, which presents the mineral in a very different fashion. When HA nucleated on the surface of CSHA sponges, the plate-like hydroxyapatite crystals appeared in small spherulitic aggregates, and these were irregular and spotty in location. In contrast, integration of hydroxyapatite throughout the collagen fibrils by using the PILP process facilitated the formation of a mesh network of interpenetrating collagen-HA mineral throughout the sponge. This was primarily a result of the capability of the PILP precursor phase to infiltrate the interstitial space within the collagen fibrils. Once this occurs, it enables the alignment of the hydroxyapatite crystals within and alongside the cylindrical fibril surface, yielding a nanostructure that reproduces that of bone. The CSPILP experimental substrates maintained the physiological ratio of inorganic to organic matter, as

determined by thermogravimeteric analysis, and thereby achieved the better representation of biological bone in comparison to the CSHA substrates.

The CSPILP substrates also provided a greater and more continuous surface area for cellular attachment. While both CSHA and CSPILP surfaces had reduced cell numbers compared to control cultures, the reduction in cell number was greatest on the collagen substrate externally coated with hydroxyapatite (CSHA). The cells likely bind preferentially to the CS and CSPILP surfaces due to the accessibility of the collagen fibrils; whereas, on the CSHA surfaces there is an increased presence of HA due to the topical coating—a condition that the cells found less favorable. On fully dense calcium phosphate substrates, reduced cell number is correlated with evidence of increased osteoblastic differentiation [12]. The greater production of osteocalcin together with the lower alkaline phosphatase activity indicates that cells on the CSHA surface differentiated to a greater degree than the cells adhered to the CSPILP surfaces. The decrease in cell growth and related increase in differentiation could largely be due to the overwhelming amount of hydroxyapatite encountered by the cells on the CSHA surface, as opposed to the more integrated and concealed exposure of HA on the CSPILP surfaces.

Cells cultured on CSPILP behaved similarly to cells cultured on collagen sponges and differently from cells cultured on CSHA, even though both CSPILP and CSHA were mineralized, and even to a higher extent in the CSPILP. The CSHA sponges exhibited a more rough topography due to mineral exposure on the surface, potentially contributing to the enhanced osteoblastic differentiation of the MG63 cells as has been

noted in studies comparing surface roughness using Ti and Ti alloy substrates [18-19], as well as bone wafers treated with osteoclasts to generate resorption pits [20].

Surface chemistry also contributed to this difference in response. CSPILP and CS sponges both presented collagen fibrils on the surface, suggesting that access to collagen is an influential factor. In order to attribute the modulation of cellular behavior to the presentation of type I collagen, we used MG63 cells that had been silenced for the α2- integrin subunit, impeding the cell's ability to bind type I collagen. Cell number was increased and osteocalcin production was reduced in the α2 silenced cells, an outcome typical of α2 silenced cell growth on TCPS, which is associated with binding to fibronectin via α5β1 [15, 20]. Cell activity is still observable in the α2-silenced MG63 cells because we achieved approximately a 70% reduction in α2- integrin subunit production of these silenced cells and not the complete ablation of the integrin which mediates some cellular binding to collagen.

We observed that osteocalcin production in the α2-silenced cells was greater for the CSPILP surfaces in comparison to CSHA surfaces. Likewise, OPG levels were decreased for CSPILP surfaces in comparison to the CSHA surfaces. Collectively, this suggests that the osteoblast-like cells are still modulated by the ratio of HA to collagen exposure, where the cells preferentially attached to the collagen even when less was accessible. α2silencing did not appreciably affect production of osteoprotegerin on the mineralized collagen sponges, although the stimulatory effect of the mineral was reduced on the sponges produced using the PILP process. This suggests that signaling via α2β1 may influence the paracrine regulatory environment. Moreover, these observations

collectively demonstrate the importance of collagen binding to osteoblast differentiation and indicate that both materials provided adequate access to collagen.

It is important to note that the source of collagen is also a critical variable in mediating cell responses. Production of osteocalcin was sensitive to whether the cells were cultured on Batch A or Batch B scaffolds, which used different commercial sources of collagen. There could be differences in crosslinking, or other processing variables we cannot ascertain. Similarly, the components of the PILP method are essential in mediating cell responses. For instance, the use of the poly-aspartate polymer to achieve the PILP method may have an unknown impact on the physiological feedback signaling mechanism of the osteoblast-like cells when interacting with the CSPILP surfaces. With this body of work, we were only able to establish a very preliminary understanding of how the inorganic and organic orientation affects a biomaterial's functionality. It is well known, however, that the inorganic and organic components of bone work in concert to facilitate mineralization, vascularization, remodeling, and overall stability of bone. While the present study indicates that cells recognize and are sensitive to the presentation of nano-biomineral and collagen, bioceramic presentation needs to be further explored to optimize cellular reaction. A biocomposite representing the physiological nature and network of bone is almost certainly able to impart the functional attributes and characteristics necessary to maintain the dynamics and stability of bone, and studies to determine if these bone-like materials can be resorbed by osteoclasts are underway. We have underscored the advantages of using the PILP method to produce viable scaffolds for bone regeneration; however, *in vivo* studies must be conducted to support the use of this methodology for clinical applications.

5.5 References

[1] Mahamid, J., Sharir, A., Addadi, L., Weiner, S., "Amorphous calcium phosphate is a major component of forming fin bones of zebrafish: indications for an amorphous precursor phase," Proc Natl Acad Sci U S A., vol 105, pp.12748-12753 (2008).

[2] Mahamid. J., Aichmayer, B., Shimoni, E., Ziblat, R., Li, C., Siegel, S., Paris, O., Fratzl, P., Weiner, S., Addadi, L., "Mapping amorphous calcium phosphate transformation into crystalline mineral from the cell to the bone in zebrafish fin rays," Proc Natl Acad Sci U S A., vol.107, pp. 316-21, (2010).

[3] Olszta, M.J., Cheng, X., Jee, S.S., Kim, Y., Kaufman, M.Y., Douglas, E.P., Gower, L.B., "Bone structure and formation: A new perspective," Mater Sci Eng R Rep., vol. 58, pp. 77-116 (2007).

[4] Weiner, S., Wagner, H.D., "The material bone: structure-mechanical function relations," Annu Rev Mat Sci., vol., 28, pp. 271-298 (1998).

[5] Boskey, A., "Mineral analysis provides insights into the mechanism of biomineralization," Calcif Tissue Int, vol. 22, pp. 533-536 (2003).

[6] Ghanaati, S., Barbeck, M., Detsch, R., Deisinger, U., Hilbig, U., Rausch, V., Sader,. R, Unger, R.E., Ziegler, G., Kirkpatrick, C.J., "The chemical composition of synthetic bone substitutes influences tissue reactions *in vivo*: histological and histomorphometrical analysis of the cellular inflammatory response to hydroxyapatite, beta-tricalcium phosphate and biphasic calcium phosphate ceramics," Biomed Mater., vol.7, (2012): 7:015005. doi:10.1088/1748-6041/7/1/015005.

[7] Duan, Y.R., Zhang, Z.R., Wang, C.Y., Chen, J.Y., Zhang, X.D., "Dynamic study of calcium phosphate formation on porous HA/TCP ceramics," J Mater Sci Mater Med., vol. 15, pp.1205-1211 (2004).

[8] Gower, L.B., Odom, D.J., "Deposition of calcium carbonate films by a polymer-induced liquid-precursor (PILP) process," J Cryst Growth., vol. 210, pp. 719-734 (2000).

[9] Bewernitz, M.A., Gebauer, D., Long, J., Colfen, H., Gower, L.B., "A metstable liquid precursor phase of calcium carbonate and its interactions with polyaspartate," Faraday Discuss, doi:10.1039/C2FD20080E (2012).

[10] Nudelman, F., Pieterse, K., George, A., Bomans, P.H., Friedrich, H., "The role of collagen in bone apatite formation in the presence of hydroxyapatite nucleation inhibitors," Nat Mater, doi: 10.1038/NMAT2875 (2010).

[11] Schwartz, Z., Fisher, M., Lohmann, C.H., Simon, B.J., Boyan, B.D., "Osteoprotegerin (OPG) production by cells in the osteoblast lineage is regulated by pulsed electromagnetic fields in cultures grown on calcium phosphate substrates," Ann Biomed Eng vol. 37, pp. 437-44 (2009).

[12] Yuan, H., et al., "Osteoinduction by calcium phosphate biomaterials," J Mater Sci Mater Med., 9(12), pp. 723-726 (1998).

[13] Begley, C.T., Doherty M.J., Hankey, D.P., Wilson, D.J., "The culture of human osteoblasts upon bone graft substitutes," Bone, vol.14, pp. 661-666 (1993).

[14] Webster, T.J., Ergun, C., Doremus, R.H., Siegel, R.W., Bizios, R., "Enhanced functions of osteoblasts on nanophase ceramics," Biomaterials, vol. 21, pp. 1803-1810 (2000).

[15] Jee, S.S, Thula, T.T., Gower, L.B., "Development of bone-like composites via the polymer-induced liquid-precursor (PILP) process. Part 1: influence of polymer molecular weight," Acta Biomater., vol. 6, pp. 3676-3686 (2010).

[16] Olivares-Navarrete, R., Raz, P., Zhao, G., Chen, J., Wieland, M., Cochran, D.L., Chaudhri, R.A., Ornoy, A., Boyan, B.D., Schwartz, Z., "Integrin alpha2beta1 plays a critical role in osteoblast response to micron-scale surface structure and surface energy of titanium substrates," Proc Natl Acad Sci, vol. 105, pp. 15767-15772 (2008).

[17] Gittens, R.A., McLachlan, T., Olivares-Navarrete, R., Cai, Y., Berner, S., Tannenbaum, R., Schwartz, Z., Sandhage, K.H., Boyan, B.D., "The effects of combined micron-/submicron-scale surface roughness and nanoscale features on cell proliferation and differentiation," Biomaterials., vol. 32, pp. 3395-403 (2011).

[18] Schwartz, Z., Olivares-Navarrete, R., Wieland, M., Cochran, D.L., Boyan, B.D., "Mechanisms regulating increased production of osteoprotegerin by osteoblasts cultured on microstructured titanium surfaces," Biomaterials vol. 30, pp. 3390-3396 (2009).

[19] Boyan, B.D., Schwartz, Z., Lohmann, C.H., Sylvia, V.L., Cochran, D.L., Dean, D.D., Puzas, J.E., "Pretreatment of bone with osteoclasts affects phenotypic expression of osteoblast-like cells," J Orthop Res., vol. 21, pp. 638-647 (2003).

[20] Keselowsky, B.G., Wang, L., Schwartz, Z., Garcia, A.J., Boyan, B.D., "Integrin alpha(5) controls osteoblastic proliferation and differentiation responses to titanium substrates presenting different roughness characteristics in a roughness independent manner," J Biomed Mater Res A., vol. 80, pp. 700-710 (2007).

CHAPTER 6

Future Directions

The ultimate goal of this dissertation was to develop a better understanding of the chemical and structural attributes that should be incorporated into a biomaterial to encourage bone formation. Identifying these features is essential when designing a composite that modulates a cell's response to the biomaterial. Analyzing the surface characteristics of human bone allowed us to determine a baseline understanding of the significant features that may play a paramount role in the formation of osseous tissue. The working hypothesis is that by incorporating the structural and chemical features we observed in human bone, into a bone substitute, we can improve cell attachment, growth, and differentiation of osteoblast cells on the biomaterial.

Mineralized collagen used as bone graft substitutes often consists of either a synthetic biomineral alone or mineral deposited on a collagen fibril surface, but normal bone consists of collagen/hydroxyapatite (HA) composites in which poorly crystalline calcium phosphate is intercalated within the fibrillar structure. With this in mind, the primary role of tissue engineered bone substitutes has been to replace lost or damaged osseous tissue while stimulating autogenous bone. This is to be achieved in concert with the resorption of the scaffolding material as it is not intended to permanently replace the bone but encourage new bone formation. There are numerous physiological advantages for using bone substitutes when biomaterials meet the necessary requirements and can achieve these desired goals. These advantages include, but are not limited to, their ability to encourage growth and differentiation of osteogenic cells, promote angiogenesis to

support the differentiated cells and newly formed tissue, as well as the substitute's potential for mass production. In this ever-evolving tissue engineering arena, the design and development of biomaterials that effectively mimic the chemical composition and micro-architecture of physiological bone is of great necessity and in great demand. With this in mind, we hypothesized that ceramic materials mimicking normal bone surface microstructure and chemistry would support an increase in osteoblast differentiation in vitro. The characterization of these materials and the evaluation of the osteoblast-like cell response to these biomaterials was the underlying premise of this work.

By characterizing human bone wafers we were able to determine that structural and chemical differences detected on bone wafer surfaces are directly related and imparted by the bone's state of mineralization. These structural and chemical attributes of mineralized, partially demineralized and fully demineralized cortical and trabecular bone dictate the osteo-surface environment and can be used as a templates for the design, processing and development of bone substitutes with varying degrees of osteoblast-like characteristics. Because the ability of inorganic and organic substances to adhere or anchor to the bone's surface is largely modulated by its surface attributes, chemical and structural characteristics of bone play a crucial role in cell attachment. A cell's surface interaction is consequently dictated by characteristics that are directly correlated and imparted by the bone's state of mineralization. The next step to further understand the chemical and structural characteristics of bone was to fully characterize the surface of cortical and trabecular bone. This step is essential in establishing the framework for which bone biomaterials should be conceptualized and modeled. Using greater variation in the states of mineralization we may be able to better understand how materials

integrate and depend on the chemical and structural components of bone. With this understanding, a more physiological and functional bone biocomposite can be formulated and designed by mapping the features elucidated into the structural and chemical design of future bone substitutes.

The chemistry of the mineral component of bone closely resembles synthetic hydroxyapatite, $Ca_{10}(PO_4)_6(OH)_2$, however the biomineral naturally occurring in bone is a nano-crystalline carbonated apatite. Moreover, the carbonate content of bone varies with the age of the individual, approximately 2-8 wt%. In our carbonated HA study, we sought out to determine the biological effects of the carbonate containing mineral on cell behavior. This study showed that nanocrystalline powders containing CO_3^{2-} can be used to generate carbonate substituted HA discs that support MG63 cell attachment, growth, and expression of proteins associated with differentiated osteoblasts. The surfaces of the discs differed structurally and chemically depending upon the original carbonate content of the nanopowders. Most importantly, we learned that cell response is sensitive to these differences. For this study, we used carbonated HA powders with 3.88wt% (C1), 4.85wt% (C2), 5.82wt% (C3); however, to more thoroughly examine the biological effects of the carbonate containing mineral on cell behavior, more carbonate HA powders should be evaluated. Carbonated HA powders ranging from 6-8wt% should also be evaluated to determine if they have more favorable biomaterial attributes.

To elucidate the exact biological role of silicate in bone formation we used tetraethyl orthosilicate and incorporated it into the hydroxyapatite (HA) lattice to produce silicate incorporated HA (Si-HA) powder. Unlike the carbonated HA discs, the silicate did not replace a phosphate or hydroxyl group, but instead was added to the lattice.

Silicate has been identified at trace levels in immature bone and is believed to play a metabolic role in new bone formation. In this study, Si-HA powders at varying concentrations were pressed into discs and used as the experimental model in order to evaluate the effect silicate incorporated HA has on osteoblast-like cell behavior.

This study demonstrated that silicate was incorporated into hydroxyapatite (Si-HA) without altering the Ca/P ratio of pure HA. Moreover, the increase in silicate concentration corresponded to an increase in percent weight of silicate for each substitute. Interestingly, the lowest Si-HA surface, 2.5wt% (S1) supported greater cell numbers but reduced differentiation compared to pure HA. Moreover, neither 6.97wt% (S2) nor 8.37wt% (S3) enhanced osteoblast differentiation compared to HA. This is in contrast to reports that silicated HA supports enhanced bone healing or that bioglasses stimulate osteoblast differentiation. This inconsistency suggests that Si content alone is not critical, but its presentation to the cells is the important factor. To further investigate the role of silicate different concentrations should be evaluated. Adjusting the macroporosity and strut porosity of the materials may also shed light on the role silicate plays in the formation of new bone. Furthermore, incorporating silicate at varying concentrations into a carbonated HA graft may yield ideal results for a bone substitute. Combining these two ionic substitutions into one bone graft material will result in a substitute that more closely mimics the chemical composition of biomineral.

In our final study, we assessed whether osteoblasts are sensitive to formatting of the mineral phase and its interaction with collagen. Human MG63 osteoblast-like cells were cultured on collagen sponges (CS) and collagen sponges mineralized with calcium phosphate using the polymer-induced liquid-precursor (PILP) process: type I collagen

fibrils are infiltrated with an amorphous mineral precursor, which upon crystallization leads to intrafibrillar HA that closely mimics physiological bone mineral (CSPILP).

In order to determine whether the collagen/mineral presentation of these composites affected osteoblast differentiation, MG63 cells stably silenced for the alpha-2 (α2) integrin subunit were used, since α2β1 integrins target collagen. Silencing α2 increased cell number on CSHA and decreased osteocalcin; cell number increased on CSPILP and osteocalcin decreased, but to a lesser extent than on CSHA. Osteoprotegerin (OPG) levels decreased in cultures of α2-silenced cells on both surfaces in comparison to OPG in wild type cells. This indicates that signaling via α2β1 mediates responses of MG63 cells to the sponges and that the cells are sensitive to formatting of the mineral phase. CSPILP surfaces in this study were created using two different sources of type I collagen due to the discontinuation of the original source of collagen used. To more fully exploit the CSPILP surfaces, the substrates using the same source of collagen should be evaluated using the same array of biological assays and compared again to the CSHA and CS surfaces. In order to create a substrate that more closely mimics normal physiological bone, future CSPILP surfaces could be designed using carbonated-HA. Substrates could also be designed to contain varying amounts of silicate incorporated into the lattice, while not replacing either the phosphate or hydroxyl groups. CSPILP surfaces closely resembling the physiological presentation of biomineral in concert with collagen may prove to be ideal biomimetic scaffolds for clinical applications.

In addition to evaluating the surface structural and chemical characteristics of bone, several other aspects such as extra-cellular matrix proteins present and the proteins that adhere to a biomaterial's surface *in vivo,* should be evaluated as well to better design

biomaterials. This work provides a preliminary understanding of some of the key features of bone that should be incorporated into the design of biomaterials upon which other key characteristics of bone should be incorporated to improve the overall functionality of biomaterials.

Vita

Brandy R. Adams

ADAMS was born in Macon, Georgia. She attended public schools in Warner Robins, Georgia, received a B.S. in Mathematics from Fort Valley State University, Fort Valley, Georgia in 2000 and a B.S.E. in Civil Engineering from Georgia Institute of Technology, Atlanta, Georgia in 2002. She later pursued and completed a doctorate in Bioengineering at Georgia Institute of Technology. Mrs. Adams enjoys traveling, cooking, and exercising in addition to researching and developing novel health concepts.